The Lightning Striking Probability for Offshore Wind Turbine Blade with Salt Fog contamination

Qingmin Li,[1,a)] Yufei Ma,[1] Zixin Guo,[1] Hanwen Ren,[1] Guozheng Wang,[2] Waqas Arif,[1] Zhiyang Fang,[3] Wah Hoon Siew[4]

[1]*State Key Lab of Alternate Electrical Power System with Renewable Energy Sources, North China Electric Power University, Beijing, 102206, China*

[2]*School of Electrical Engineering, Shandong University, Jinan, 250061, China*

[3]*Sinomatech Wind Power Blade Co., Ltd, No.66 Xi Xiao Kou Rd., 100192, Beijing, China*

[4]*Department of Electronic & Electrical Engineering, the University of Strathclyde, Glasgow, G1 1XQ, UK*

The blades of offshore wind turbine are prone to be adhered with salt fog after long-time exposure in the marine-atmosphere environment, and salt fog reduces the efficiency of lightning protection system. In order to study the influence of salt fog on lightning striking probability (LSP), the lightning discharge process model for wind turbine blade is adopted in this paper considering the accumulation mechanism of surface charges around salt fog area. The distribution of potential and electric field with the development of downward leader is calculated by *COMSOL Multiphysics LiveLink for MATLAB*. A quantitative characterization method is established to calculate the LSP base on the average electric field before return stroke and the LSP distribution of blade is shown in the form of graphic view. Simulation results indicate that the receptor and conductor area close to receptor the area are more likely to get struck by lightning, and the LSP increases under the influence of salt fog. The validity of the model is verified by experiments. Furthermore, the receptor can protect the blade from lightning strikes effectively when the lateral distance between rod electrode and receptor is short. The influence of salt fog on LSP is more obvious if salt fog is close to receptor or the scope of salt fog area increases.

I. INTRODUCTION

The first offshore wind turbine of the world was installed in 1990 in Nogersund, Sweden. In the following 20 years, Denmark, Sweden, the Netherlands and the UK have built a number of demonstration offshore wind power projects which were mainly funded by the Government and research institutions. After dramatic growth of onshore wind power from first round of concession in 2003, China has also initiated the first round of national-level offshore wind farm concession projects in 2010. The turbine capacity increases from 567 MW in 2003 to nearly 13,803MW in 2009 in China[1]. It is foreseeable that offshore wind power development will boom dramatically in the future all over the world.

[a)] Electronic-mail: lqmeee@ncepu.edu.cn.

However, the damage caused by lightning striking remains the biggest threat to wind turbines[2]. Statistics show that about 5.56 wind turbine blades are damaged by lightning striking for every 100 blades per annum on average. The lightning protection for offshore wind turbines meets more severe challenges. Offshore wind turbines are installed in open environment with high tower and salt fog could adhere to the surface of blade easily under marine-atmosphere environment. The above factors will affect the protection efficiency of lightning protection system (LPS) for offshore wind turbine blades.

In order to improve the protection efficiency of current LPS, it is vital to discover the area with high probability to be struck by lightning on blade surface. Field observation indicated that approximate 90% of lightning strikes on blade surface within 5m from blade tip[3] in failure cases. Some researchers obtained the details of lightning propagation process, such as lightning leader characteristics by lightning local systems (LLSs), optical observation techniques and high-speed photography. Zeng[4] summarized the recent progress on lightning physics and lightning protection research, including lightning observation, lightning initiation, lightning downward leader propagation, lightning attachment and return stroke, etc. Lu[5] studied the connecting behavior of the downward and upward leaders during the attachment process preceding the first return stroke by high-speed video images. However, the observation methods also encountered challenges due to long experimental period and lack of the observation stations for wind power farms. Some researchers carried out long air gap experiments to study the distribution of attachment points on blade installed with different kinds of receptors[6-8]. Long[9] analyzed the protection area of receptors based on self-consistent leader inception and propagation model. However, current researches are lack of the quantitative characterization for lightning striking probability on blade surface.

In the marine-atmosphere environment, wind turbine blades are prone to be adhered with salt fog. Yokoyama[10] found that soluble and non-soluble contaminants such as dust, sand and salt deposited on the blade surface would enhance the surface discharge activity. The research carried by Douar[11] indicated that pollution deposit on the surface of insulator reduces the flashover voltage, irrespective of the polarity of applied voltage. Kumar[12] found that flashover voltage reduced with the increasing of salt deposit density on GFRP material, and the flashover voltage under negative switching impulse is less compared with positive switching impulse. However, the influence mechanism of salt fog in various positions and scopes to the distribution of lightning attachment points is not clear.

This paper discusses the quantitative characterization of lightning striking probability (LSP) distribution of wind turbine blade and the influence of salt fog on the LSP based on the achievements from charged particles

accumulation and long gap discharge areas. It will be a theoretical basis on making effective lightning protection measures and painting advanced marine antifouling coatings for offshore wind turbine blades.

II. LIGHTNING DISCHARGE PROGRESS MODEL FOR WIND TURBINE BLADE

Les Renardierers Group proposed that the natural lightning discharges showed some similarities with the laboratory long gap discharges based on the experimental studies[13-16] and the observation results obtained by K. Berger[17], given as follows.

1) Both share the same physical process. The development of a natural lightning is initialized and sustained by the formation of 'streamer corona' and 'leader' discharges, very similar to those observed in the laboratory long gap discharges[18];
2) The lightning attachment point is influenced by the development of both the downward and upward leaders;
3) For both natural lightning discharge and laboratory long gap discharge, the critical electric field for initializing an upward leader is roughly the same, with the approximate value of 500kV/m.

Actually, it is impossible to conduct a natural lightning discharge experiments in the lab due to restricted space and lack of background conditions. Based on the similarity theory proposed by Les Renardierers Group, the laboratory long gap discharge experiments are widely used to study the attachment process for natural lightning discharges.

Two typical test setups recommended in IEC 61400-24[19] are appropriate for the tests on the complete blades used for design development and verification. Each test arrangement is intended to initialize electrical activities such as corona, streamers and leaders, at the targeted specimen just before a lightning attachment may happen. Yokoyama[20] used a 12MV high voltage impulse generator at Shiobara testing yard of Central Research Institute of Electric Power Industry to investigate the lightning attachment manner to the wind turbine blades. Three-meter long blade-sample was cut from an actual twelve-meter long wind turbine blade made of GFRP. He found that the discharges progressed along the surface of a blade-sample tip and attached to the receptor in many cases, and sometimes the discharges passed through the air and attached to the receptor directly. Radičević[21] used the typical 3MW 1:40-scaled wind turbine model, with an arching high-voltage electrode under different modes of stationary and rotating blades, to study the physical mechanism of the blade rotation influence on the wind turbine in triggering lightning discharges. It was found that, the breakdown voltage decreased and the connection point of the leader approached the blade tip with an increasing blade speed.

Considering the above research advances, the laboratory long gap discharge experiment can be an efficient method to investigate the attachment process for the natural lightning discharges.

A. Simplified model of wind turbine blade

The structure of wind turbine blade is shown in Fig. 1(a). The blade is made of glass fiber reinforced plastic (GFRP) and equipped with LPS including a tip receptor and copper stranded conductor. Generally, the length of operational offshore wind turbine blade is more than 45m, and the computation complexity will increase if a whole blade model is adopted. In order to reduce computation complexity and time, a simplified wind turbine blade is adopted as shown in fig. 1(b). The blade body of simplified model is made of GFRP, with relative permittivity of 4.0, and the size is 400×200×3mm. An aluminum-made receptor is installed at the tip of blade, with the size of 20×200×3mm, and it is connected to the ground through a copper conductor.

Salt fog could be easily adhered to the blade surface, and the main constituent of the salt fog is water soluble salt, such as NaCl. Increasing salt fog contamination will attach to the wind turbine blade after long-time exposure in the marine-atmosphere environment, and the shape of the salt fog contamination renders random style. In order to facilitate the modeling process while ensuring universality and generality of the proposed model, a cylindrical salt fog contamination model located at the coordinates (0.1, 0.05) is adopted in the paper, as shown in Fig. 2.

Setting the center point of the underside of blade as the starting point of coordinates, a coordinate system is established in this paper, as shown in Fig. 3. The height of external electrode of 0.2m, the distance between the electrode bottom and blade upper surface is assumed to be 0.4m in the simulation model.

B. Charge distribution along the stepped downward leader

Both experimental and physical modeling have proven that the charge density along the leader channel shows an increasing trend as the leader propagates[22-23]. The stepped downward leader is assumed to develop towards the direction with maximal electric field intensity. The electric field intensity along downward leader is 50kV/m.

For a stepped leader without branch channels shown in Fig. 4, the charge distribution in the stepped leader is expressed as followed[24]:

$$\rho_l = \rho_0 + kL = k \times \frac{H_c - h}{\cos\theta} \tag{1}$$

$$Q_{tip} = fQ_c = \frac{1}{2} fk \times \left(\frac{H_c - h_{tip}}{\cos\theta} \right)^2 \tag{2}$$

Where ρ_l is the charge density in the leader channel section; ρ_0=0 is the charge density at starting point of the stepped leader channel; Q_{tip} is the charge in the leader tip; Q_c is the total charge in the leader channel section; L

is the leader channel length; H_c is the height of external electrode; h is the height above ground of the stepped leader; θ is the angle between stepped downward leader and vertical axis; h_{tip} is the height of the stepped leader tip; k is a coefficient to describe the relation between ρ_l and L, and it increases almost linearly with the first return stroke peak current I_p, which can be written as: k=3.8×10^{-9}I_p.; f is a correlation coefficient to describe the relation between Q_{tip} and Q_c.

C. Accumulation mechanism of surface charge on salt fog

The electric field $\boldsymbol{E}$ depends on the electric potential φ. The relationship between potential and charge density ρ is described by the Possion Equation:

$$\boldsymbol{E} = -\nabla\varphi \tag{3}$$

$$\nabla^2\varphi = -\frac{\rho}{\varepsilon_0} \tag{4}$$

Considering the geometry of salt fog shown in Fig. 5, the polarization vector $\boldsymbol{P}_1$, $\boldsymbol{P}_2$ in air and salt fog can be calculated as:

$$\begin{cases} \boldsymbol{P}_1 = \varepsilon_0(\varepsilon_g - 1)\boldsymbol{E}_1 \\ \boldsymbol{P}_2 = \varepsilon_0(\varepsilon_{sf} - 1)\boldsymbol{E}_2 \end{cases} \tag{5}$$

Where ε_g is the relative permittivity of air. ε_{sf} is the relative dielectric constant of salt fog, which can be estimated with the single Debye relaxation law[25].

The net surface charge density δ_i at the upper surface of the salt fog[26] is expressed as following:

$$\delta_i = |\boldsymbol{P}_2| - |\boldsymbol{P}_1| = \varepsilon_0(\varepsilon_{sf} - 1)|\boldsymbol{E}_2| - \varepsilon_0(\varepsilon_g - 1)|\boldsymbol{E}_1| \tag{6}$$

Free charge at the interface δ_f is expressed as followed:

$$\delta_f = |\boldsymbol{D}_2| - |\boldsymbol{D}_1| = \varepsilon_0\varepsilon_{sf}|\boldsymbol{E}_2| - \varepsilon_0\varepsilon_g|\boldsymbol{E}_1| \tag{7}$$

Where $\boldsymbol{D}_1$, $\boldsymbol{D}_2$ is the displacement vector of air and salt fog respectively.

Eliminating $\boldsymbol{E}_2$ from equation (6) and (7), the net surface charge density δ_i can be calculated as:

$$\delta_i = \delta_f\left(\frac{\varepsilon_{sf} - 1}{\varepsilon_{sf}}\right) + E_1\varepsilon_0\left(\frac{\varepsilon_{sf} - \varepsilon_g}{\varepsilon_{sf}}\right) \tag{8}$$

Plenty of charged particles are distributed in the salt fog area intensively under the influence of background potential.

D. The initiation and progression of upward leader near wind turbine blade

Numerous charged particles are accumulated near wind turbine blade with the propagation of downward

leader, and the distribution of electric field is distorted by accumulated charges. Corona will incept when the quantity of charges exceeds critical value N_{cri}[27].

$$\exp\left(\int_0^R [\alpha(E)-\eta(E)]dx\right) > N_{cri} \tag{9}$$

Where R is boundary region of charges collision where $\alpha=\eta$; α is impact ionization coefficient; η is adhesion coefficient; x is the distance between tip of corona and electrode; $N_{cri}=0.55\times10^8$ is the critical value.

Based on the simplified physical model proposed by Becerra and Cooray[28], the propagation of stepped-upward leader is simulated in this paper, as shown in Fig. 6. The distribution of potential U_1 is changed to $U_2^{(0)}$ after the formation of corona. l_{ldr} is the length of leader stem and $l_{str}^{(0)}$ represents the tip of corona area. The total corona charge, $\Delta Q^{(0)}$, can be calculated by:

$$\Delta Q^{(0)} = K_Q \cdot \int_{l_{ldr}}^{l_{str}^{(0)}} \left(U_1(l) - U_2^{(0)}(l)\right) \cdot dl \tag{10}$$

Where K_Q is the geometric factor describing, with a typical value of 3.5×10^{-11} C/V m. An unstable upward leader will incept once the space charges within corona area reach 1μC.

The potential at the tip of upward leader $U_{tip}^{(i)}$ can be calculated by:

$$U_{\text{tip}}^{(i)} = l_{ldr}^{(i)}E_\infty + x_0 E_\infty \ln\left[\frac{E_{\text{str}}}{E_\infty} - \frac{E_{\text{str}}-E_\infty}{E_\infty}\times\exp\left(-\frac{l_{ldr}^{(i)}}{x_0}\right)\right] \tag{11}$$

Where E_∞ is the electric field of the final quasi-stationary leader, with the value of 50kV/m. x_0 is the product of development velocity of upward leader and the time constant. E_{str} is the electric field of negative streamer[29-30], with the value of 450kV/m.

The total corona charge at the tip of leader for each step, $\Delta Q^{(i)}$, can be calculated by:

$$\Delta Q^{(\text{i})} = K_Q \int_{l_{ldr}^{(i)}}^{l_{str}^{(\text{i})}} \{U_{tip}^{(\text{i}-1)} - [U_{tip}^{(i)} + E_{str}(l - l_{ldr}^{(i)})]\} dl \tag{12}$$

Where U_{tip} is the potential at the tip of upward leader.

The integral expression represents the shades area shown in Fig. 6. The length of upward leader at the $(i+1)^{th}$ step can be calculated by:

$$l_{ldr}^{(i+1)} = l_{ldr}^{(i)} + \frac{\Delta Q^{(i)}}{q_L} \tag{13}$$

Where q_L is a constant that denotes the charge per unit length necessary to achieve the thermal transition from the diffuse glow to the upward leader channel.

E. Attachment process of lightning discharge

Average electric field between downward leader tip and potential lightning attachment points is calculated as:

$$E_{av} = \frac{U_{down} - U_{up}}{d} \tag{14}$$

Where U_{up} is electric potential of potential lightning attachment points on the surface of blade; U_{down} is electric potential of downward leader tip; d is the distance between two points.

The breakdown electric field of air gap is 3 000 kV·m^{-1} under uniform electric field. The breakdown voltage reduces with the increasing of non-uniformity of electric field. The final attachment is assumed to occur when one of the following conditions is satisfied:

1) E_{av} between the downward leader tip and potential striking points on blade exceeds 2 000kV/m;

According to [18], the electric field conditions, in which an electrical discharge may develop and propagate in the air gap, will change by orders of magnitude with the gap length. In small gaps (millimeter range) the electric field required for a breakdown is around 3 000 kV·m^{-1}, while in larger gaps (up to 1 meter) it would be five times lower, around 500 kV·m^{-1}. The distance between the head of a downward leader and the blade sample decreases to less than 0.4m with subsequent development of the downward leader. Hence, a critical valve value of 2 000kV/m is assumed after fitting electric field curve for initializing a breakdown.

2) E_{av} between the downward leader tip and upward leader tip exceeds 500kV/m[24].

The calculation flow chart is shown in Fig. 7.

III. THE POTENTIAL DISTRIBUTION AND LIGHTNING STRIKING PROBABILITY OF WIND TURBINE BLADE

A. The distribution of potential nearby wind turbine blade

To solve the nonlinear differential equation system, suitable boundary conditions must be defined on the electrode and blade sample. As shown in Fig. 3, the electric potential on the external electrode U_{HV} and on the receptor and conductor U_{GND} is assigned as a Dirichlet condition:

$$U_{\mathrm{HV}} = 300kV \tag{15}$$

$$U_{\mathrm{GND}} = 0 \tag{16}$$

AC/DC module of COMSOL Multiphysics is used to simulate the distribution of electric potential nearby wind turbine blade by solving Possion Equation. In order to implement the complex iterative calculation shown in Fig. 7 and simplify the data processing, *COMSOL Multiphysics LiveLink for MATLAB* is used for numerical

computation.

The distribution of potential nearby wind turbine blade of section *xz* (y=0) is shown in Fig. 8, and the blade sample area is magnified for better visualization. The potential distribution nearby blade is asymmetry in space due to the special structure of LPS for wind turbine blade. The potential near the receptor is more distorted.

Under the influence of strong electric field intensity, the air surrounding the electrode will get ionized. Downward leader will get incepted if the voltage applied to external electrode is high enough. The stepped downward leader is assumed to develop towards the direction with maximal electric field intensity at a certain step length. The final attachment will occur if the conditions introduced in Section II (A) are satisfied.

B. The lightning striking probability of blade surface

The randomness and transience of lightning discharge process causes the uncertain distribution of lightning attachment points. However, the lightning striking probability is influenced by the average electric field intensity. The stronger electric field intensity means the higher probability to get struck by lightning. In the paper, P_{ls}, expressed as followed, is adopted to evaluate the possibility of each area on wind turbine blade to get struck by lightning.

$$P_{ls} = E_{av} / E_{\max} \tag{17}$$

Where E_{av} is the average electric field between downward leader tip and potential lightning attachment point on the surface of blade; E_{max} is the maximum electric field intensity; P_{ls} is the lightning striking probability of the area on blade surface.

Fig. 9(a) shows the 3D map of lightning striking probability on blade surface. The high altitude area is more likely to get struck by lightning. Fig. 9(b) shows the contour plot of lightning striking probability on blade surface. The area of $P_{ls} \geq 0.9$ is prone to get struck by lightning.

The area with high probability to get struck is mainly distributed in the middle position of receptor and conductor area nearby receptor. The lightning striking probability around area, with the coordinates of (0.1, 0.05), increases under the influence of salt fog.

When it comes to the arc-shaped blade model, the same conclusions can be obtained. So the quantitative characterization method established in the paper has universality, and it won't be influenced by the shape of blade.

According to [31], the physical process of surface charge distribution on the blade surface includes three parts: electric conduction along the surface of the blade, electric conduction within the gas volume, and electric

conduction through the volume of the blade. The electric conduction through the volume of the blade is expressed as $J_I = \frac{\partial D}{\partial t} + \gamma_V \cdot E$, which is influenced by the conductivity γ_V, and the electrical conductivity of salt fog contamination area is larger than the other areas on the blade body. So more charged particles will be accumulated in the salt fog contamination area.

A corona will incept when the quantity of charges exceeds a critical value for corona discharge. The corona promotes the ionization of the air nearby the salt fog contamination area. As shown in Fig. 10, positive charges move towards the salt fog area under the influence of the background electric field, and plenty of negative charges are distributed in the air gap. According to the Possion Equation, the potential nearby salt fog area decreases under the influence of negative charges. According to Equation 14 and 17, the average electric field between downward leader and the area nearby salt fog will increase, and the LSP will increase under influence of the salt fog contamination.

The vertical cutting lines (VCLs) on blade surface with the abscissa of x=-0.2m, -0.1m, 0m, 0.1m and 0.2m is shown in Fig. 11(a). The LSP along the VCLs is shown in Fig. 11(b). For the lightning striking probability along the same cutting line, the area nearby conductor (y=0m) is more likely to get struck by lightning. Because the conductor is connected to the ground, and the potential nearby conductor is distorted more seriously than blade body.

The horizontal cutting line (HCL) across salt fog area with the ordinate of y=0.5m is shown in Fig. 11(a). The LSP along HCL is shown in Fig. 12. The simulation result indicates that the LSP of the area with the abscissa of 0.1m increases 0.016 approximately under the influence of salt fog.

IV. EXPERIMENTAL VERIFICATION

A. Experiment setup

The setup of experiment platform is shown in Fig. 13. The positive standard 1.2/50μs lightning impulse is applied to the external electrode. The size and relative position of experimental sample is consistent with the simulation model shown in Fig. 3. The external electrode is just above the blade sample, and the distance between electrode and upper surface of sample is 0.4m. The woven fabric glass fiber reinforced plastics sample with the size of 400×200×3mm is selected for carrying out the experimental study. The surface of sample is wiped with anhydrous ethanol before experiment. The aluminum-made receptor is installed at the head of blade, and connected to the ground through conductor. The salt fog is prepared with NaCl, $MgCl_2$, $MgSO_4$ and $CaCl_2$ by mixing them with demineralized water, concentration of each composition is shown in TABLE. 1. The salt

fog is smeared on the certain area of blade surface to form a thin layer, as shown in Fig. 13(b). The size and relative position of salt fog is consistent with the model shown in Fig. 2.

TABLE 1 Composition and concentration of artificial sea water

Composition	NaCl	$MgCl_2$	$MgSO_4$	$CaCl_2$
Concentration(g/L)	24.53	5.20	4.09	1.16

B. Positive lightning discharge experiment results

The positive standard 1.2/50μs lightning impulse with the amplitude of 300kV is applied to the electrode. Discharge experiments are conducted for 25 times in the case of clean blade and blade smeared with salt fog respectively. The discharge process can be captured by digital camera by long-exposure. The typical discharge paths are shown in Fig. 14. For blade smeared with salt fog, the lightning attachment points are distributed in (1) the area below electrode, (2) receptor area and (3) the area smeared with salt fog, as shown in Fig. 14(a), 14(b) and 14(c) respectively. While for clean blade, the lightning attachment points are distributed in (1) the area below electrode and (2) receptor area, as shown in Fig. 14(d) and 14(e). Lightning strikes on the area nearby receptor 2 times, and then flashovers from attachment point to receptor through blade surface, as shown in Fig. 14(f).

Statistical analysis is conducted according to the experimental photographs. The distribution of lightning attachment points is shown in Fig. 15. For blade smeared with salt fog, lightning discharges strike on Area I, II and III 5 times, 15 times and 5 times, constituting 25%, 50% and 25% of the total lightning discharges respectively. For clean blade, lightning discharges strike on Area I and II 4 times and 19 times, constituting 16% and 76% of the total lightning discharges. For the blade sample smeared with salt fog, the lightning strikes 12 times on the middle position of receptor, and strikes 3 times on both side of receptor.

Compared with the experimental observations and the simulation results shown in Fig. 9, the conclusion is consistent in the following 3 aspects:

1) The receptor and conductor area nearby receptor is more likely to be struck by lightning;

2) More lightning might strike on the middle position of receptor than the both side;

3) Under the influence of salt fog, the lightning striking probability of the area smeared with salt fog increases to some extent.

V. THE INFLUENCE OF EXTERNAL FACTORS TO LIGHTNING STRIKING PROBABILITY

A. The influence of the position of external electrode on LSP

The observations[32-33] indicate that the lateral distance (LD) between lightning leader and the object struck

by lightning is diverse due to the randomness of lightning discharge. In order to analyze the influence of the position of external electrode on LSP, the rod electrode is installed along X-axis in turn, with the coordinates of (0, 0, 0.4), (0.1, 0, 0.4), (0.2, 0, 0.4) and (0.3, 0, 0.4) respectively, as shown in Fig. 16. The amplitude of voltage applied to the electrode is the same in each simulation.

The LSP of blade surface under different positions of external electrode is shown in Fig. 17, where x_{ed} is the abscissa of the electrode.

For the case of x_{ed}=0m, the electrode is far away from receptor and close to the blade body. The areas of high probability to be struck by lightning are mainly distributed in the middle position of receptor area and conductor area with the abscissa from 0.08m to 0.2m. For the case of x_{ed}=0.1m and x_{ed}=0.2m, the areas of high probability to be struck by lightning are distributed in the receptor area and conductor area close to the receptor. For the case of x_{ed}=0.3m, the areas of high probability to be struck by lightning are distributed in the receptor area. The simulation results indicate that the receptor installed at blade tip could protect the blade from being struck by lightning effectively when the lateral distance between rod electrode and receptor is short.

TABLE. 2 shows the LSP of 1) blade smeared with salt fog, with the coordinate of (0.1, 0.05, 0.003), and 2) the same area of clean blade under different x_{ed}. Compared with the case of x_{ed}=0.2m and x_{ed}=0.3m, the LSP of the area smeared with salt fog is higher when x_{ed}=0 m and x_{ed}=0.1m because that the external electrode is closer to the salt fog area and the average electric field between electrode and salt fog is stronger.

TABLE 2 The comparison of LSP under different x_{ed}

x_{ed}(m)	LSP of the area smeared with salt fog	LSP of the same area of clean blade
0	0.715	0.699
0.1	0.687	0.666
0.2	0.614	0.603
0.3	0.505	0.500

B. The influence of the position of salt fog on LSP

Each point on the blade surface of offshore wind turbine might be adhered with salt fog. In order to analyze the influence of the position of salt fog on LSP, typical positions, with the coordinates of (-0.1, 0.05, 0.003), (0, 0.05, 0.003), (0.1, 0.05, 0.003) and (0.2, 0.05, 0.003), are selected in the paper, as shown in Fig. 18. All other parameters are kept constant.

The lightning striking probability along the HCL, shown in Fig. 11(a), under different positions of salt fog is shown in Fig. 19, where x_{sf} is the abscissa of the salt fog. The comparison of LSP under different x_{sf} is shown in TABLE 3.

The calculated results indicate that the impact of salt fog on LSP is significant in the case of x_{sf}=0.1m and

x_{sf}=0.2m. The potential nearby receptor area is distorted more seriously due to the special structure of lightning protection system for wind turbine blade, as shown in Fig. 8. More negative charged particles will be gathered nearby salt fog area if the electric field is stronger. So the impact of salt fog on LSP is more obvious when salt fog is closer to the receptor.

TABLE 3 The comparison of LSP under different x_{sf}

x_{sf}(m)	LSP of the area smeared with salt fog	LSP of the same area of clean blade
-0.1	0.358	0.353
0	0.512	0.505
0.1	0.715	0.699
0.2	0.881	0.873

C. The influence of the scope of salt fog on LSP

The increasing salt fog will be attached to the wind turbine blade after long-time exposure in the marine-atmosphere environment, and the scope of the salt fog has the impact on the LSP. In order to analyze the influence of the scope of salt fog on LSP, three cylindrical salt fog models, with the radius of 0.01m, 0.02m and 0.05m respectively, is adopted in the simulation, as shown in Fig. 20. The other simulation conditions are the same.

The lightning striking probability of the HCL, shown in Fig. 11(a), under different radius of salt fog is shown in Fig. 21, where r is the radius of the salt fog.

With salt fog of cylindrical radius r=0.01m, r=0.02m and r=0.05m, the LSP increases 0.016, 0.031 and 0.103 respectively. For the case of r=0.05m, the LSP of the salt fog area increases from 0.699 to 0.802, which indicates that more lightning might strike on that area. As shown in Fig. 20, the salt fog area is close to receptor and conductor area when the radius of salt fog increases. The electric field nearby receptor and conductor is larger compared with other area on blade body. Equation 8 shows that the density of surface charge increases with the increasing of electric field intensity. The accumulation of negative charged particles will reduce the potential around salt fog area. Therefore, the impact of salt fog on LSP is more obvious when wider area is attached with the salt fog.

VI. CONCLUSION

Simulation and experiment about lightning discharge process are conducted to study the lightning striking probability of the offshore wind turbine blade attached with salt fog under different external conditions. In this paper, the following conclusions have been drawn.

1. A computational model of the lightning striking probability (LSP) based on the average electric field is

proposed in this paper. The area of P_{ls}≥0.9 is prone to get struck by lightning. The validity of the model is verified by observation results of lightning discharge experiments under laboratory conditions.

2. Both simulation and experimental results indicate that the LSP increases under the influence of salt fog attached to the blade surface.
3. The area with high probability to get struck by lightning is mainly distributed in the receptor area and conductor area close to receptor. The tip receptor could protect the blade from being struck by lightning effectively when the lateral distance between rod electrode and receptor is short.
4. The impact of salt fog on LSP is more significant when salt fog is closer to the receptor area. So the area nearby receptor is suggested to be painted with advanced marine antifouling coatings.
5. The increasing salt fog will be attached to the wind turbine blade after long-time exposure in the marine environment, and LSP will increase if more area is attached with salt fog. Therefore, the blades of offshore wind turbine should be cleaned at regular intervals.

ACKNOWLEDGMENTS

This work was supported by National Natural Science Foundation of China (51420105011) and the Fundamental Research Funds for the Central Universities (2016XS06).

REFERENCE

[1]D. Zhang, X. Zhang, *et al*, Renew. Sustain. Energy Rev. 15, 4673 (2011).
[2]Z. Guo, Q. Li, J. Yan, *et al*, Journal of Electrical Engineering, 5, 10 (2015).
[3]A. C. Garolera, PhD thesis, Tehcnical University of Denmark, 2014.
[4]R. Zeng, C. Zhuang, X. Zhou, *et al*, High Voltage, 1, 2 (2016).
[5]W. lu, Q. Qi, Y. Ma, *et al*, High Voltage, 1, 11 (2016).
[6]N. J. Vasa, T. Naka, S. Yokoyama, *et al*, in ICLP2006, Kanazawa, Japan, 1483 (2006).
[7]S. Arinaga, K. Tsutsumi, N. Murata, et al, in ICLP2006, Kanazawa, Japan, 1493 (2006).
[8]A. M. Abd-Elhady, N. A. Sabiha, M. A. Izzularab, Electric Power Systems Research, 107, 133 (2014).
[9]M. Long, M. Bceerra, R. Thottappillil, in ICLP2016, Estoril, Portugal, (2016).
[10]S. Yokoyama and N. J. Vasa, in ICLP2004, Avignon, France, 936 (2004).
[11]M. A. Douar, A. Mekhaldi and M. C. Bouzidi, IEEE Trans. Dielectr. Electr. Insul. 17, 1284 (2010).
[12]V. Sathiesh Kumar, Nilesh J. Vasa, *et al*, IEEE Trans. DEI, 21, 2283 (2014).
[13]Les Renardieres Group, Electra, 23, 53 (1972).
[14]Les Renardieres Group, Electra, 35, 47 (1974).
[15]Les Renardieres Group, Electra, 53, 31 (1977).
[16]Les Renardieres Group, Electra, 74, 67 (1981).
[17]K. Berger, Bull. Schweiz. Elektrotech, 63, 21403 (1972).
[18]I. Gallimberti, G. Bacchiega, *et al*, Comptes Rendus Physique, 3, 1335 (2002).
[19]IEC 61000-24: 2010 Wind turbine generator systems - Part 24：Lightning protection, IEC, 2010.
[20]S. Yokoyama, Electric Power Systems Research, 94, 3 (2013).
[21]B. M. Radičević, M. S. Savić, *et al*. Energy, 45, 644 (2012).
[22]V. Cooray, V. Rakov and N. Theethayi, Journal of Electrostat. 65, 296 (2007).
[23]Mingli Chen, Dong Zheng, Yaping Du, Yijun Zhang, J. Geophys. Res. 118, 4670 (2013).
[24]W. Shi, Q. Li, L. Zhang, J. Appl. Phys. 116, 101303-1 (2014).
[25]T. Meissner, F.J. Wentz, IEEE Trans. Geosci. Remote Sens. 42, 1836 (2004).
[26]J. S. Shrimpton, IEEE trans. Dielectr. Electr. Insul, 12, 573 (2005).
[27]M. Abdel-Salam, A. A. Turky, A. A. Hashem, J. Phys. D: Applied Physics, 31, 2550 (1998).
[28]M. Becerra, V. Cooray, IEEE Trans. on Power Delivery, 21, 897 (2006).
[29]Y. Ma, L. Zhang, *et al*, Proceedings of the CSEE, 36, 5975 (2016).
[30]W. Shi and Q. Li, Proceedings of the CSEE, 34, 2470 (2014).
[31]G. Ma, H. Zhou, *et al*, IEEE Trans. Dielectr. Electr. Insul., 22, 3312 (2015).
[32]W. Lv, L. Chen, *et al*, J. Geophys. Res. 117, D19211 (2012).
[33]Y. Zhang, W. Lv, *et al*, High Vol. Eng. 34, 2022 (2008).

Figure captions

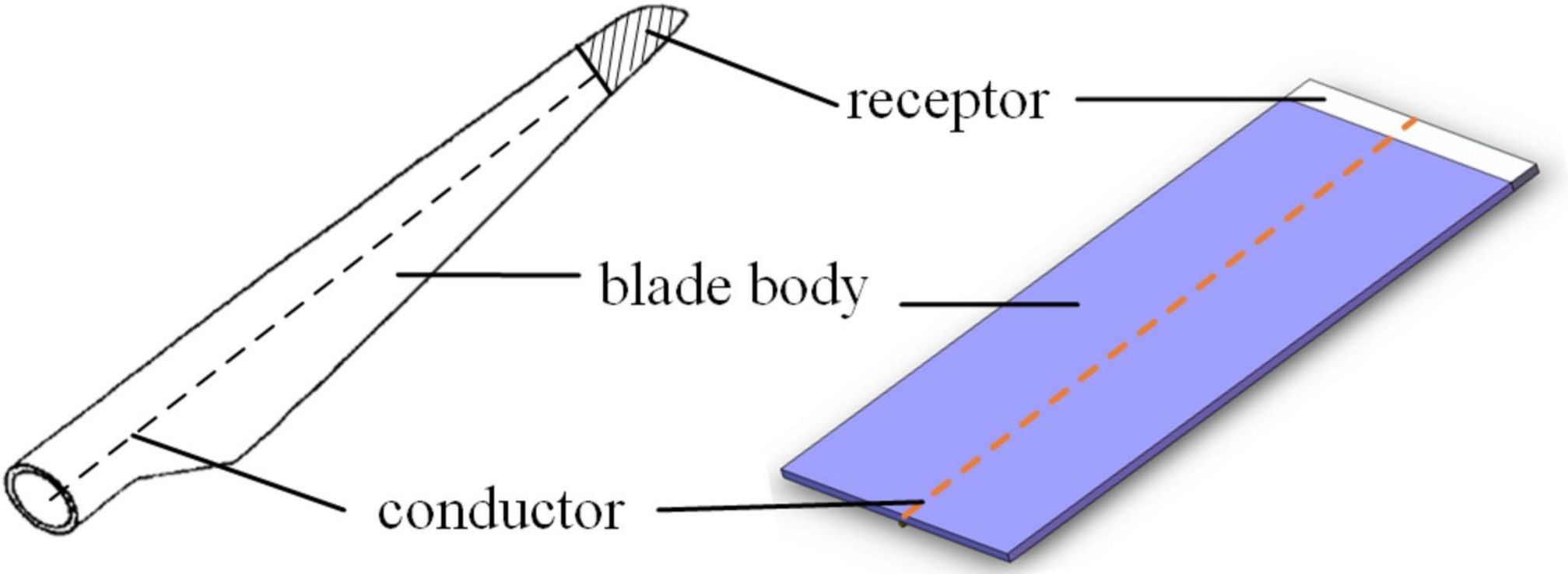

(a) The structure of wind turbine blade

(b) The simplified model of wind turbine blade

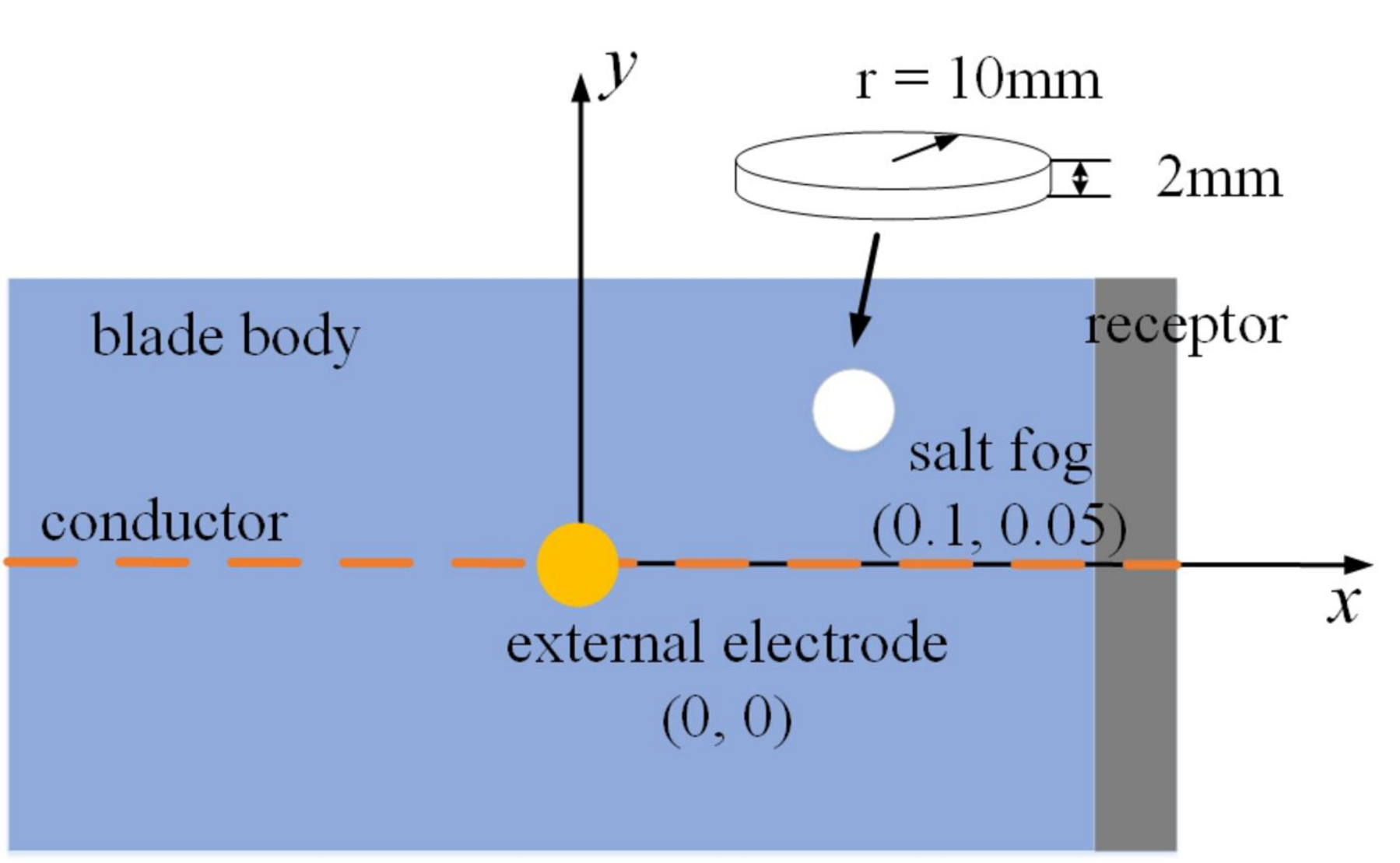
y
r = 10mm
2mm
blade body
receptor
salt fog
(0.1, 0.05)
conductor
x
external electrode
(0, 0)

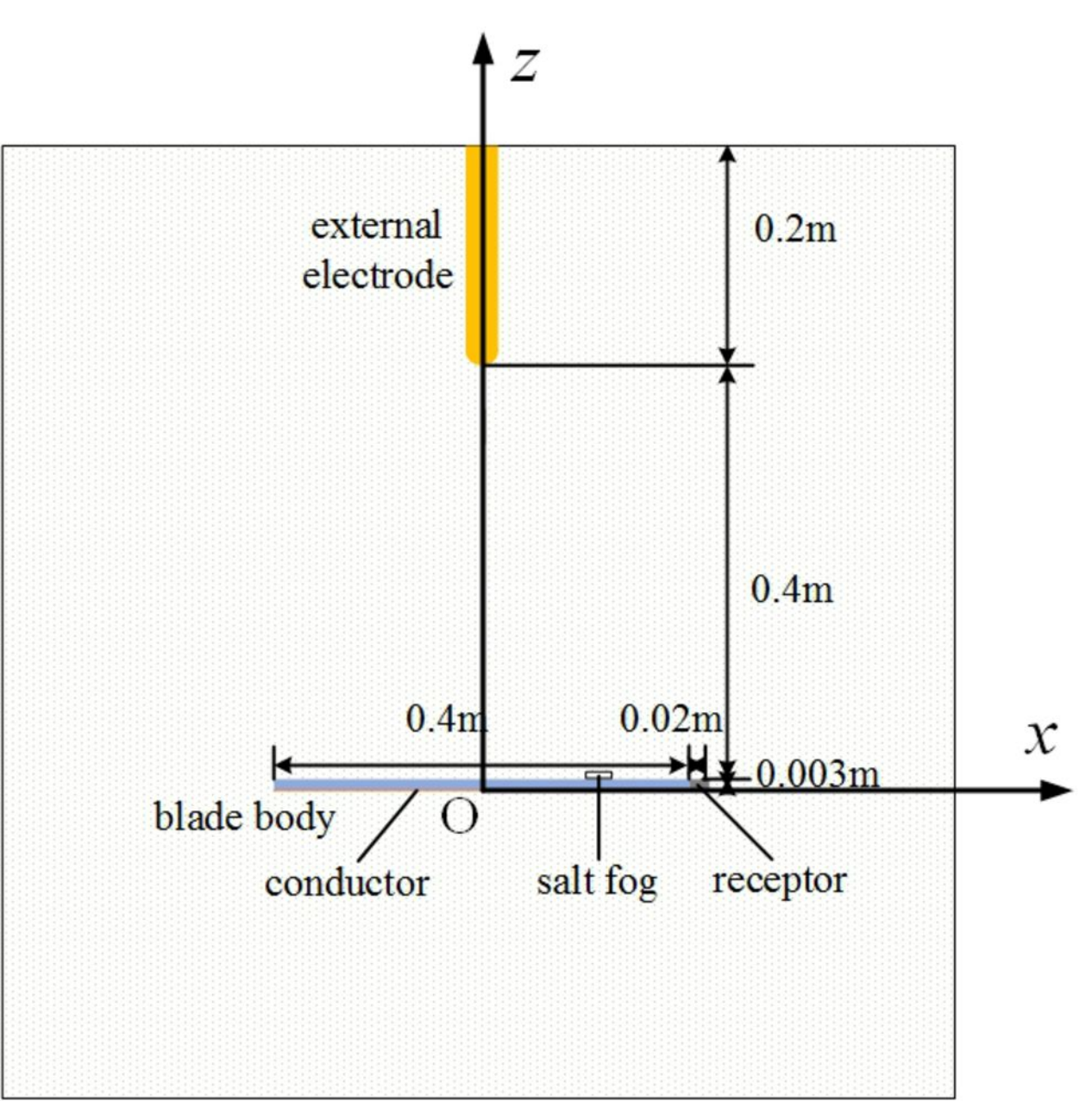
z
external
electrode
0.2m
0.4m
0.4m
0.02m
0.003m
x
blade body
O
conductor
salt fog
receptor

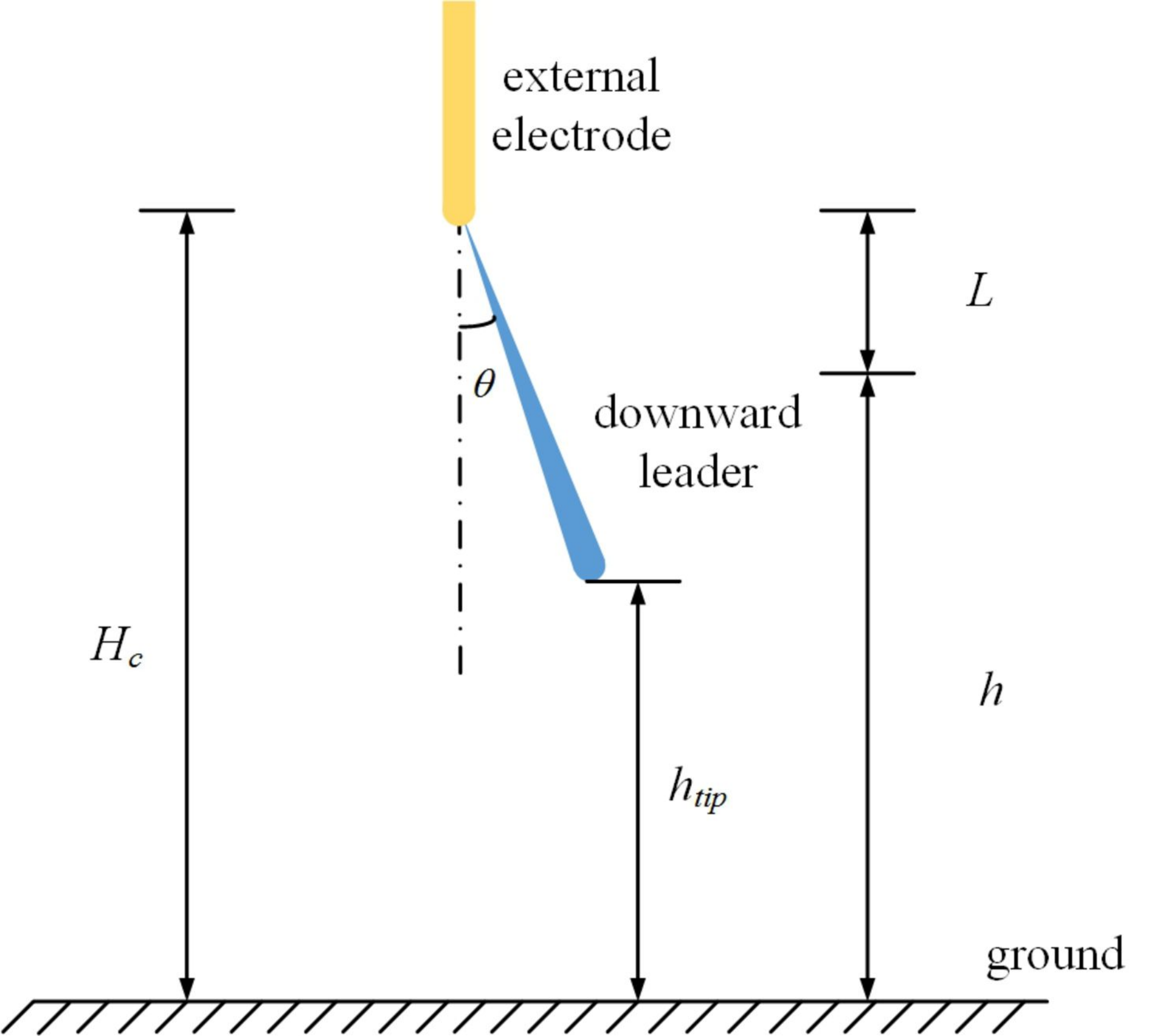
external
electrode
L
θ
downward
leader
H_c
h
h_{tip}
ground

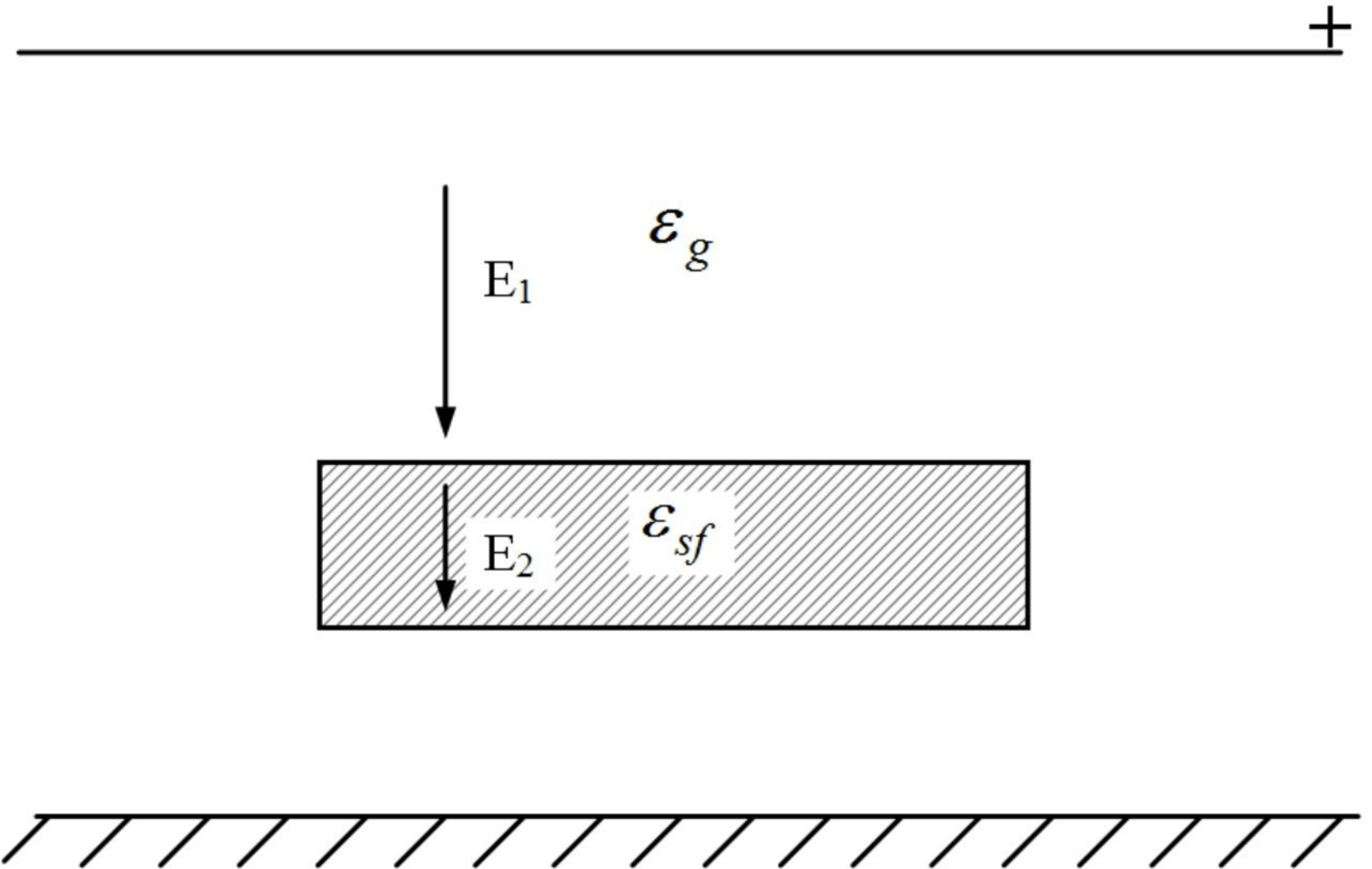
+
ε_g
E_1
E_2
ε_{sf}

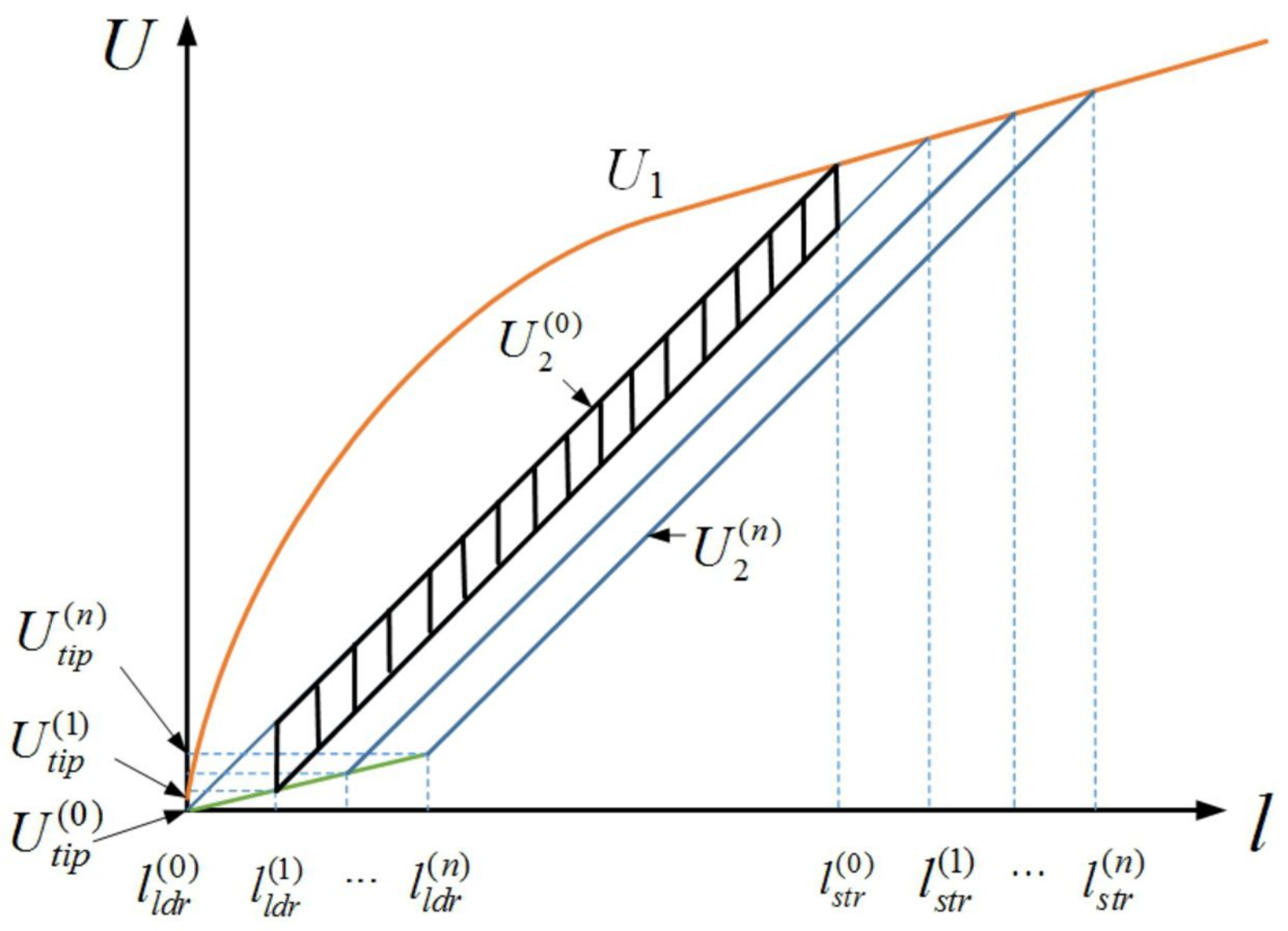
U
U1
U2(0)
U2(n)
Utip(n)
Utip(1)
Utip(0)
l
ldr(0)
ldr(1)
...
ldr(n)
lstr(0)
lstr(1)
...
lstr(n)

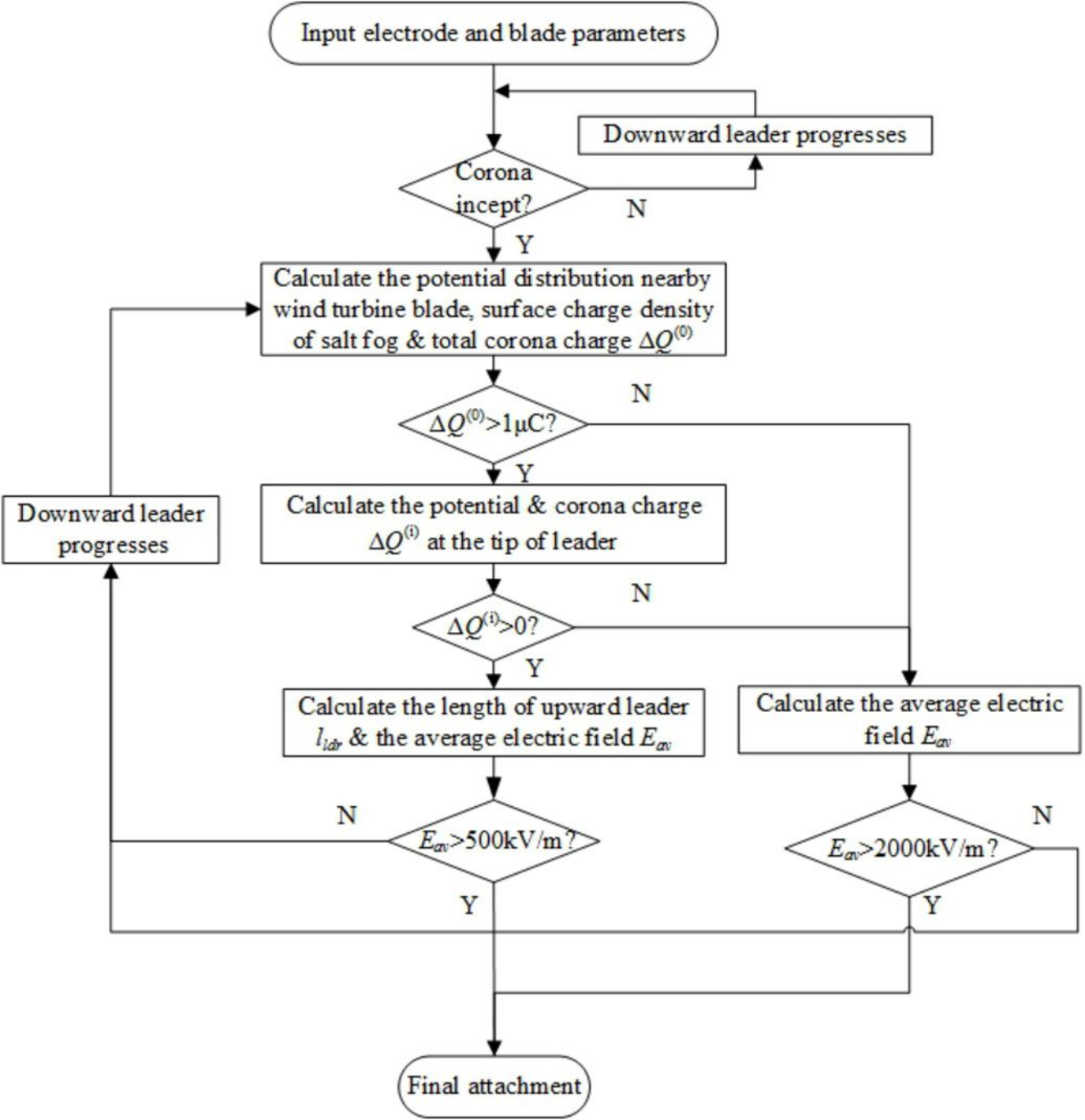
Input electrode and blade parameters
Downward leader progresses
Corona incept?
N
Y
Calculate the potential distribution nearby wind turbine blade, surface charge density of salt fog & total corona charge $\Delta Q^{(0)}$
N
$\Delta Q^{(0)}$>1μC?
Y
Downward leader progresses
Calculate the potential & corona charge $\Delta Q^{(i)}$ at the tip of leader
N
$\Delta Q^{(i)}$>0?
Y
Calculate the length of upward leader l_{ldr} & the average electric field E_{av}
Calculate the average electric field E_{av}
N
E_{av}>500kV/m?
Y
N
E_{av}>2000kV/m?
Y
Final attachment

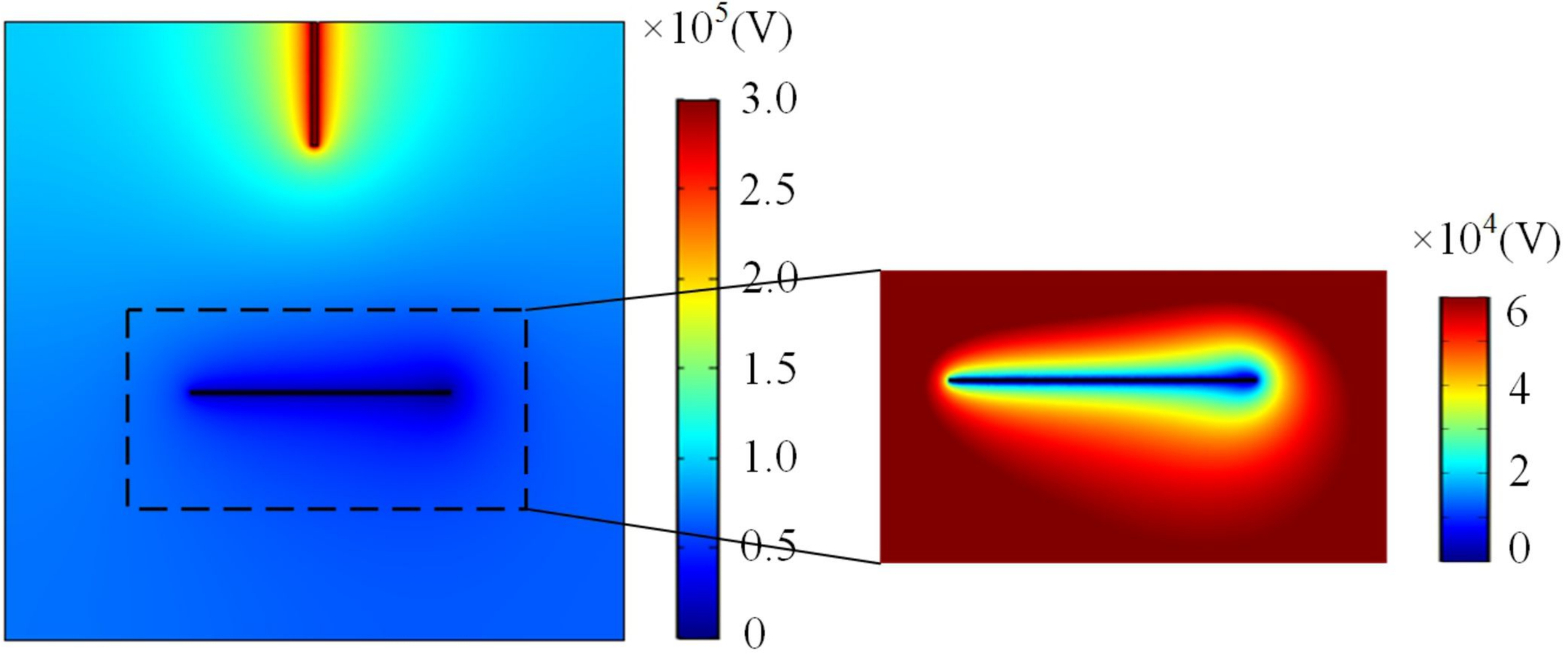
×10^5(V)
3.0
2.5
2.0
1.5
1.0
0.5
0
×10^4(V)
6
4
2
0

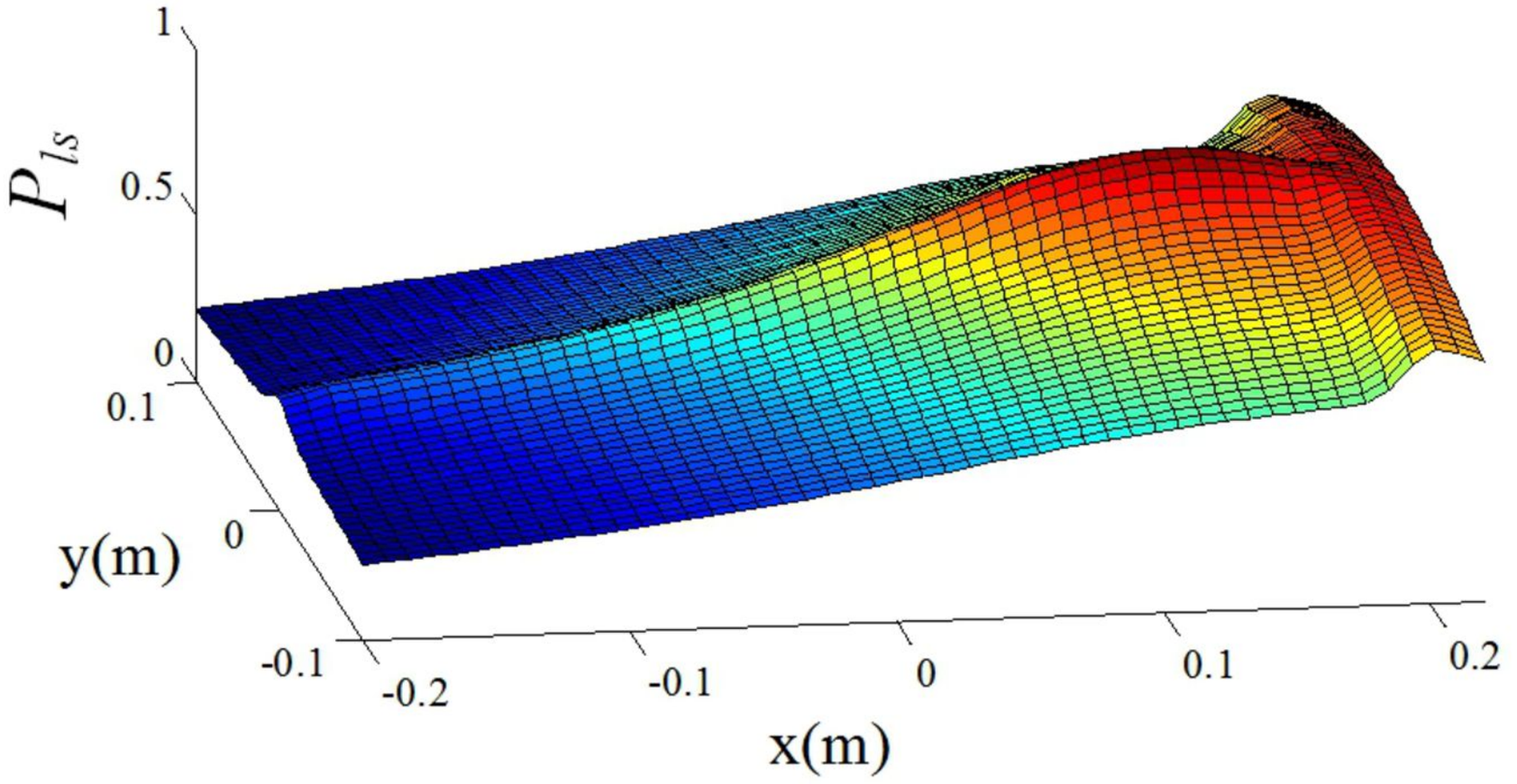

(a) 3D map of LSP on blade surface

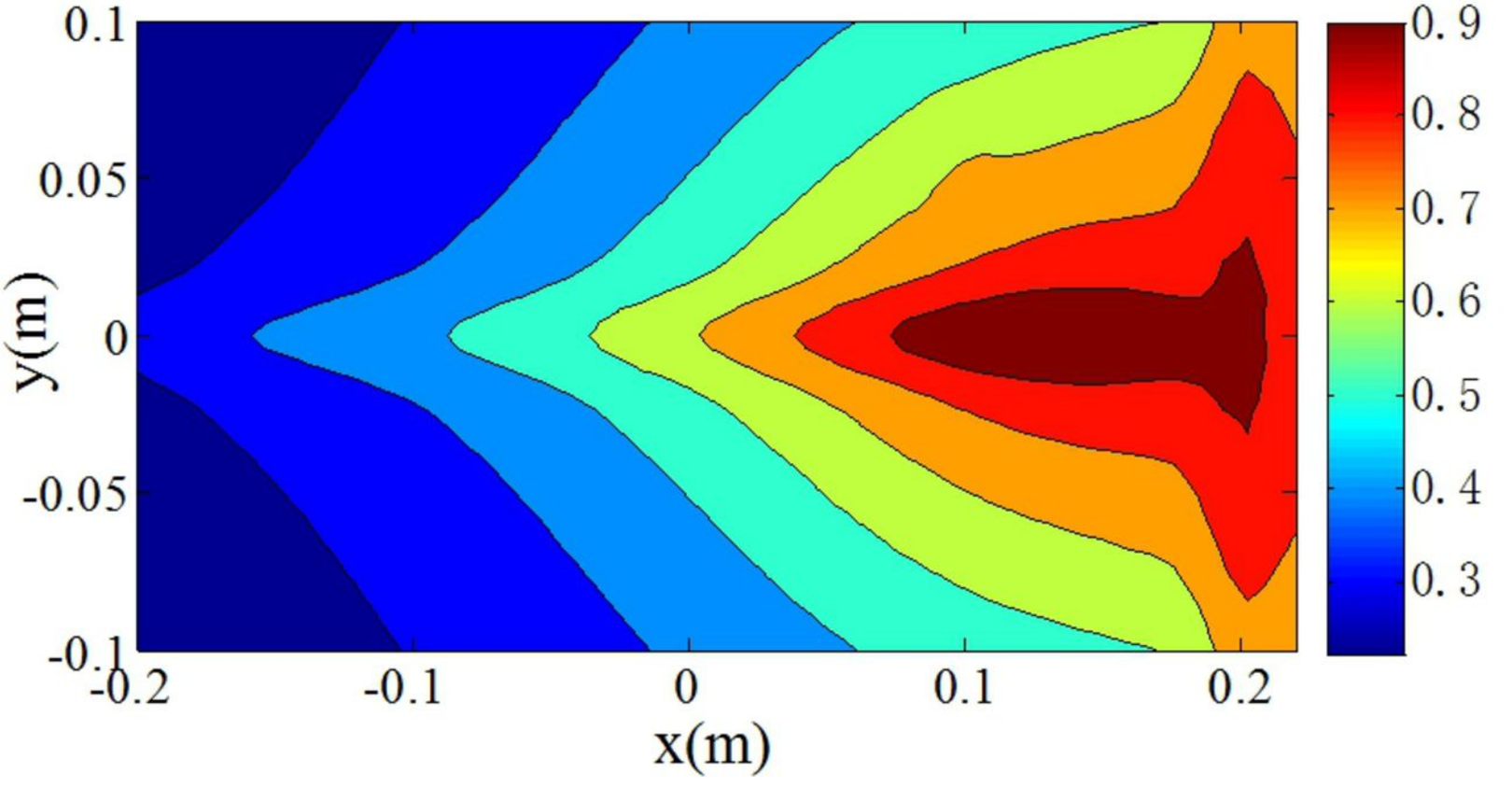

(b)The contour plot of LSP on blade surface

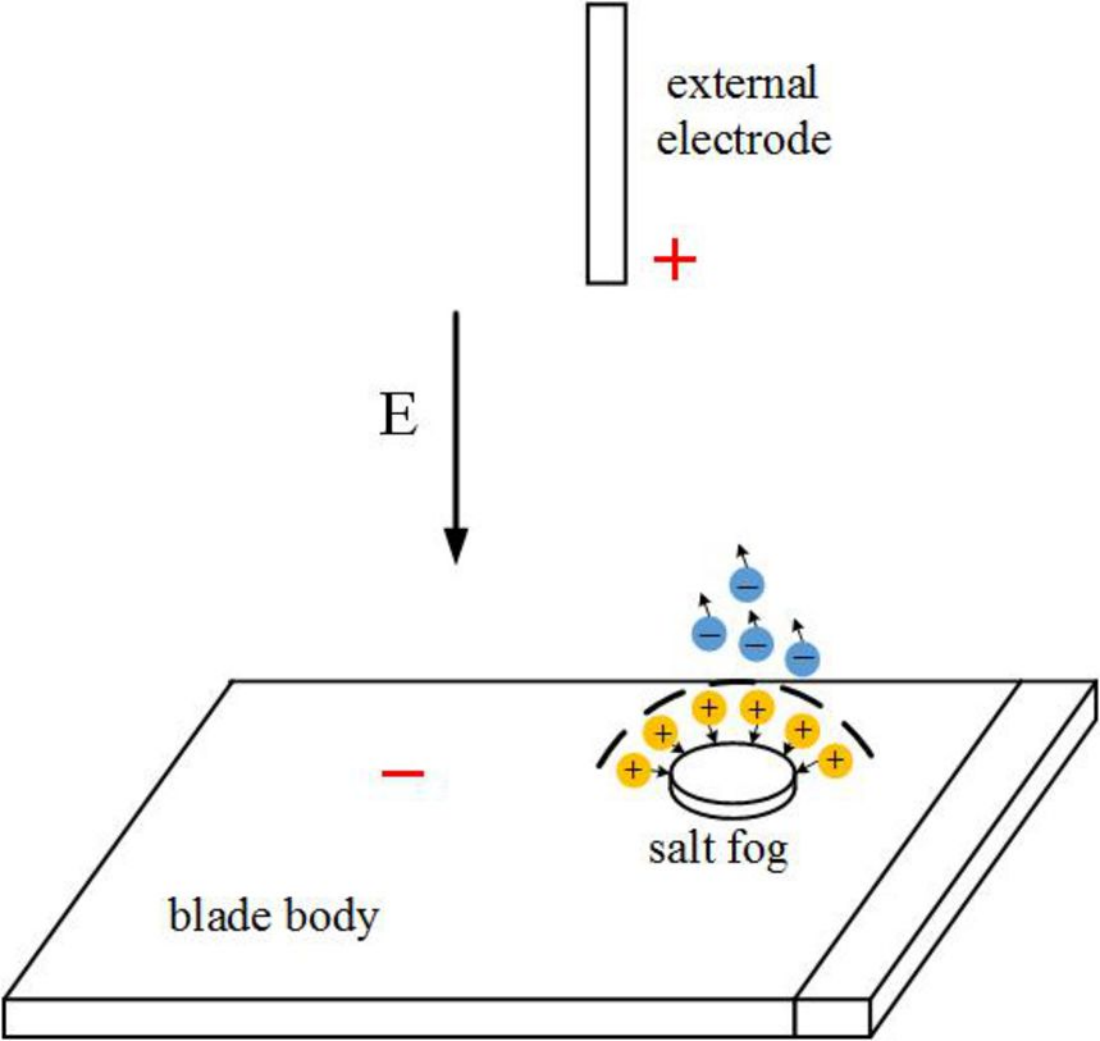
external
electrode
+
E
−
salt fog
blade body

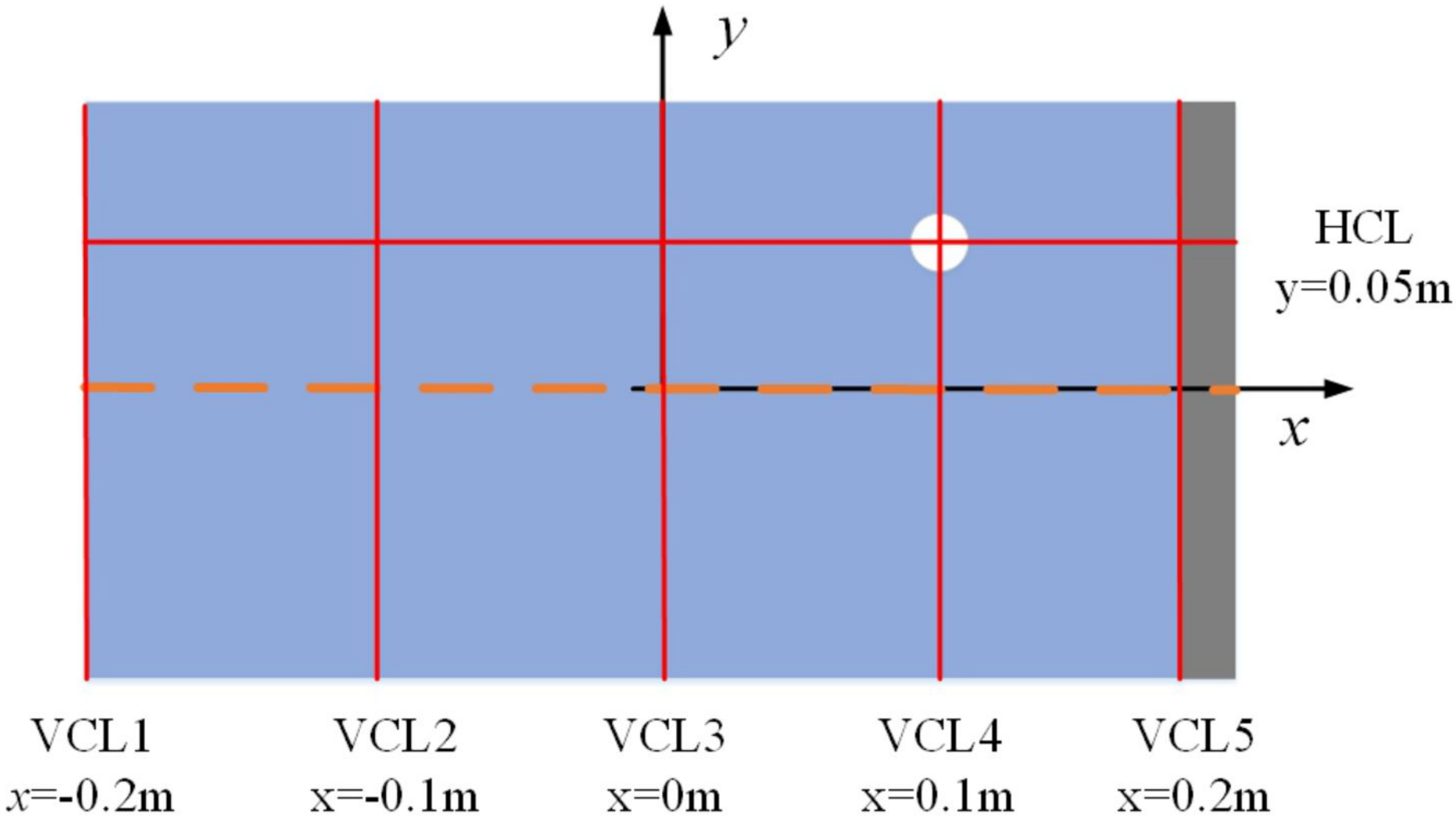

(a) Schematic diagram of the VCL and HCL

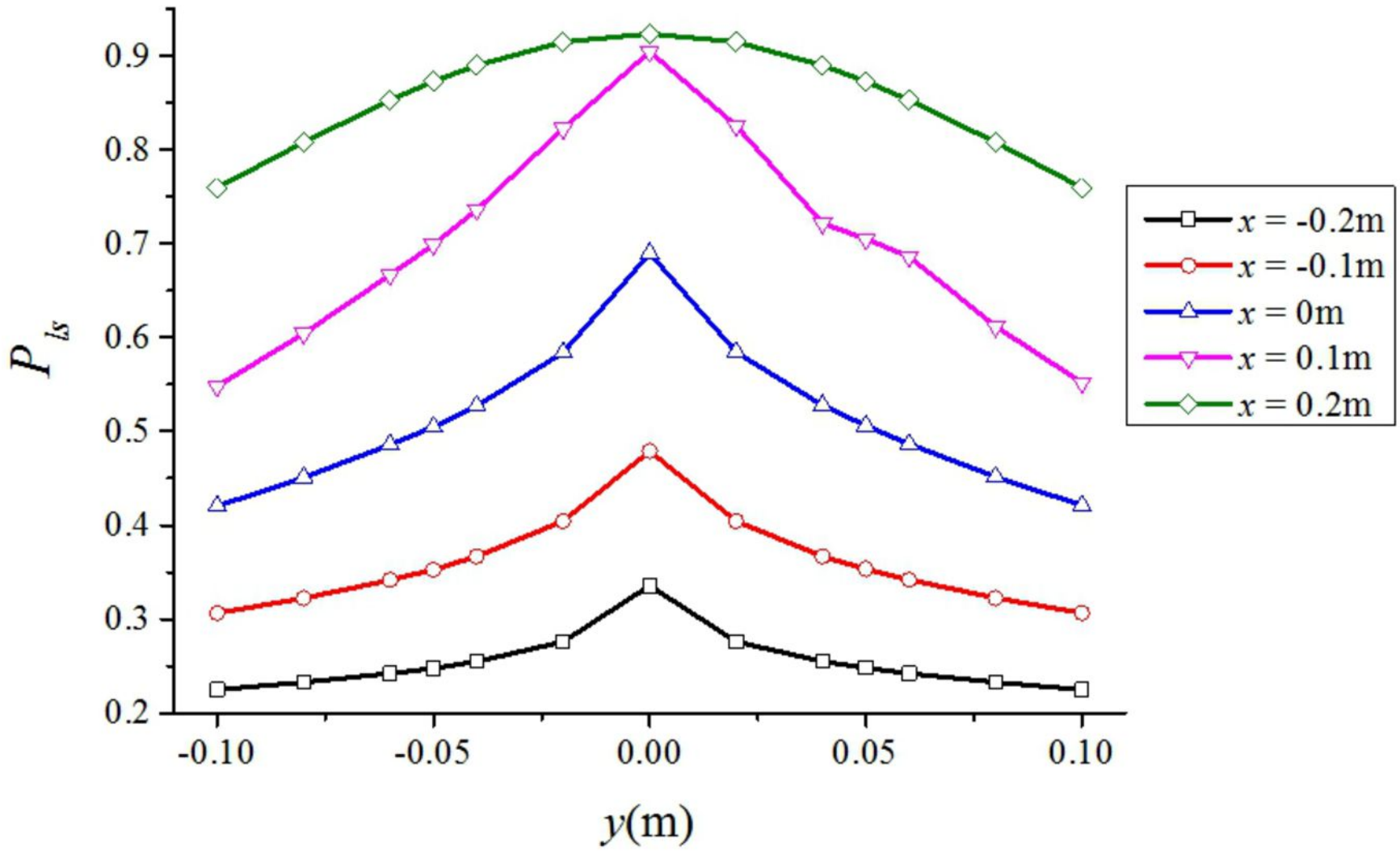

(b) LSP along the vertical cutting lines

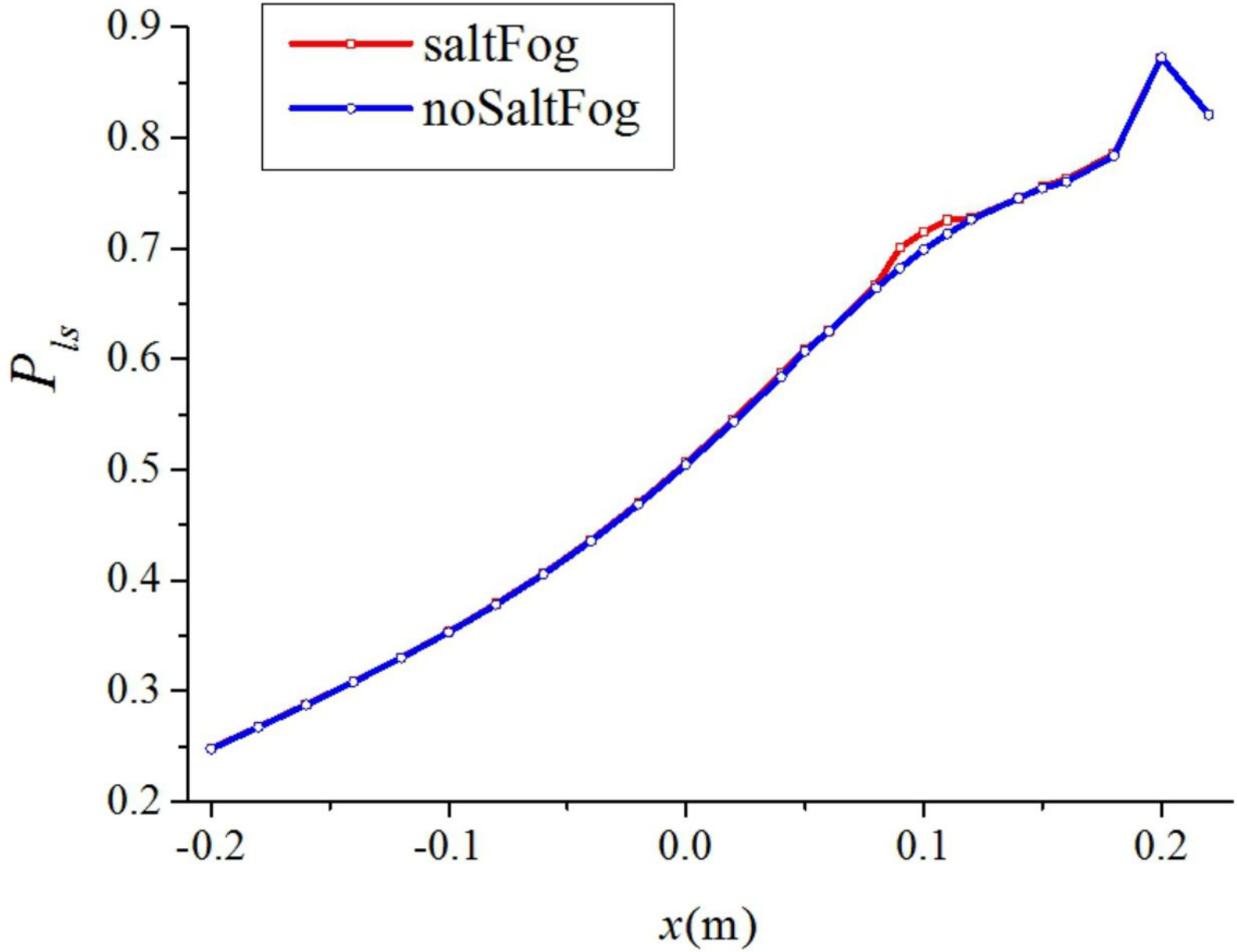
saltFog
noSaltFog
0.9
0.8
0.7
0.6
0.5
0.4
0.3
0.2
P_{ls}
-0.2
-0.1
0.0
0.1
0.2
x(m)

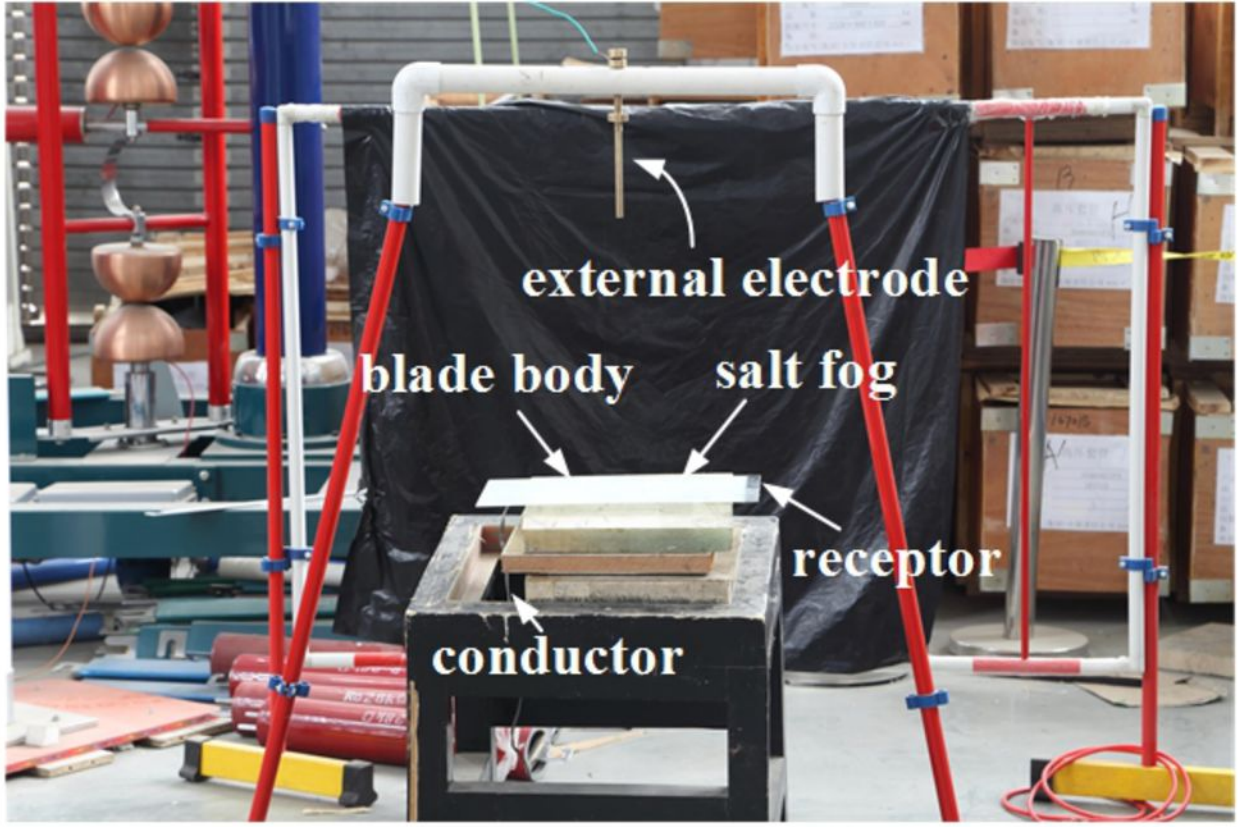

(a)The front view of experiment platform

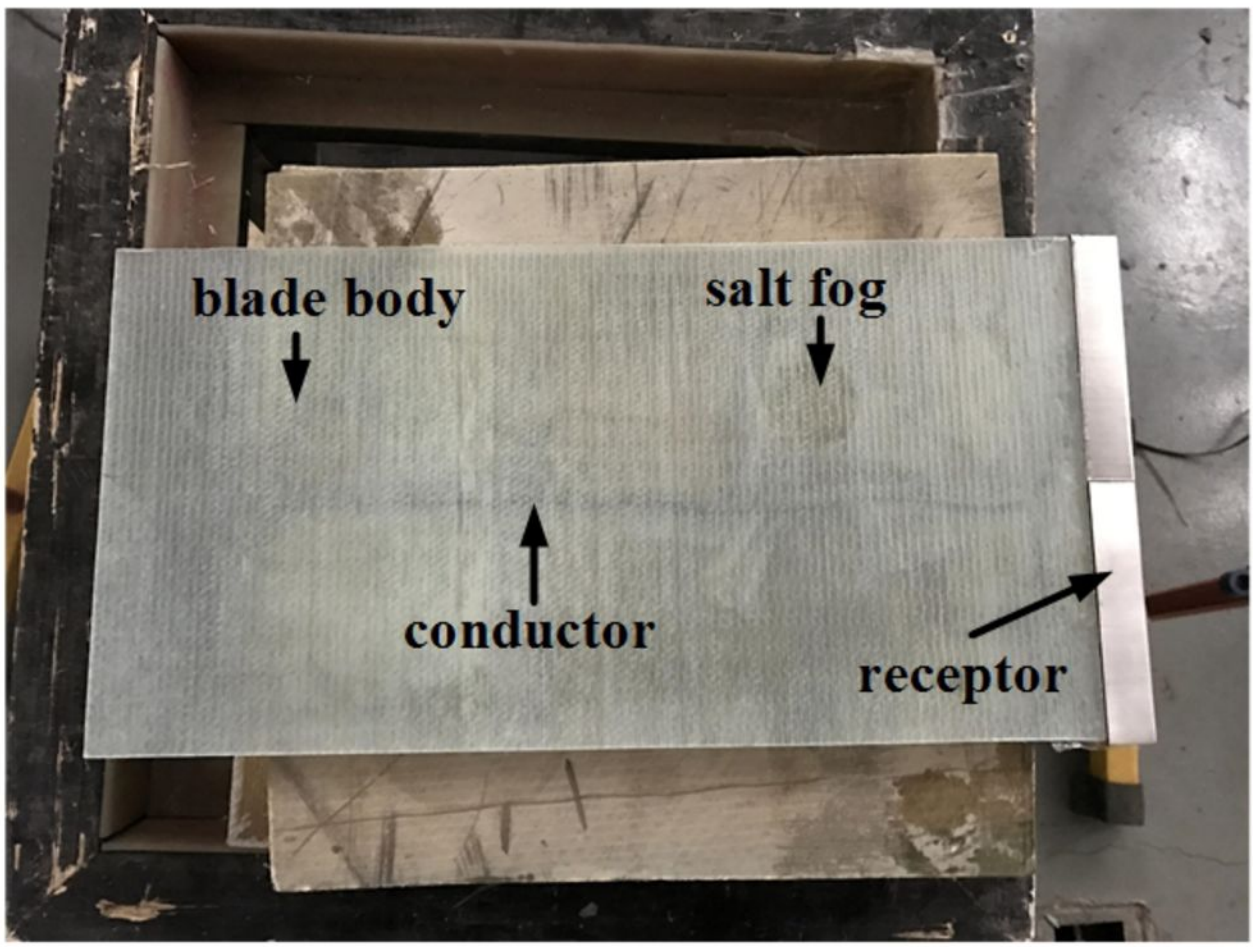

(b) The vertical view of blade sample

(a) smeared with salt fog,
area below external electrode

(b) smeared with salt fog,
receptor area

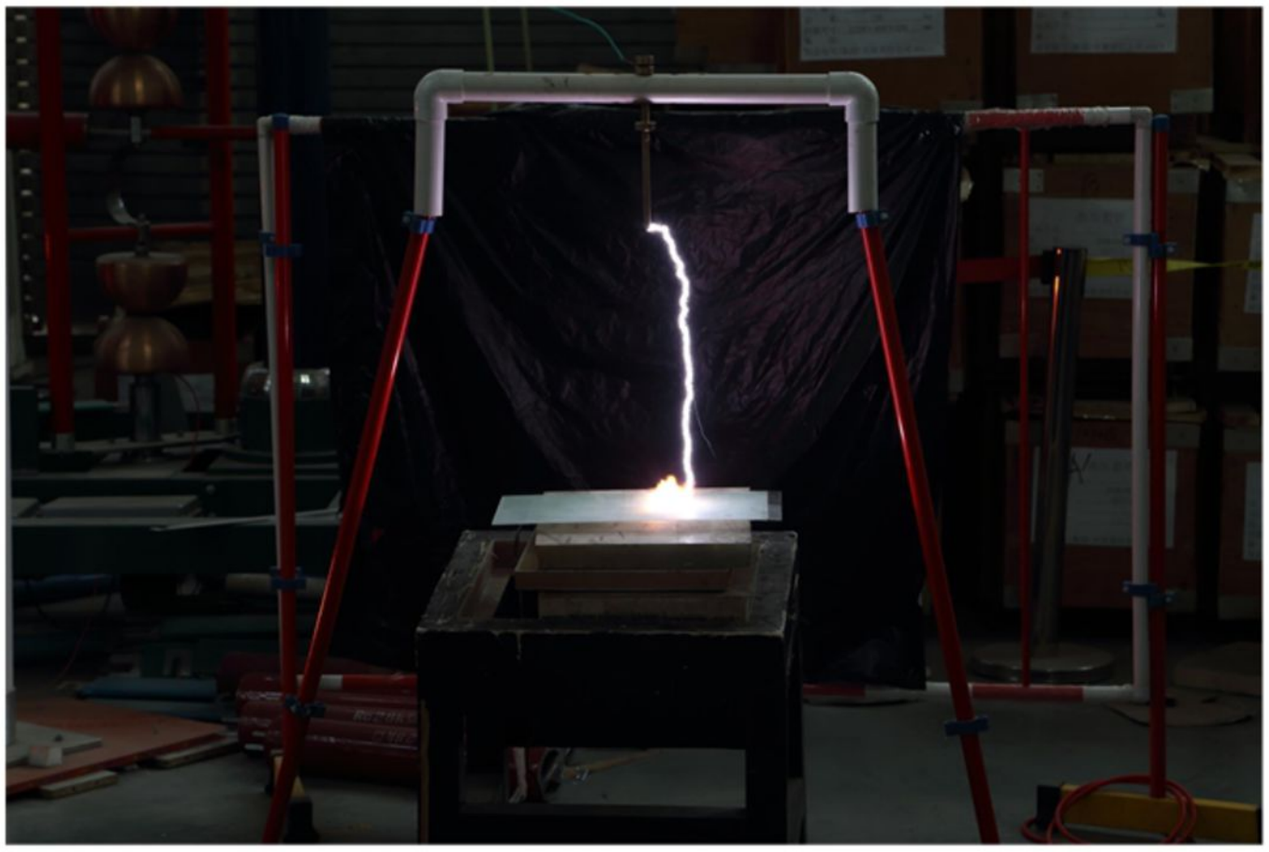

(c) smeared with salt fog,
salt fog area

(d) clean blade,
area below external electrode

(e) clean blade,
receptor area

(f) clean blade,
conductor area nearby receptor

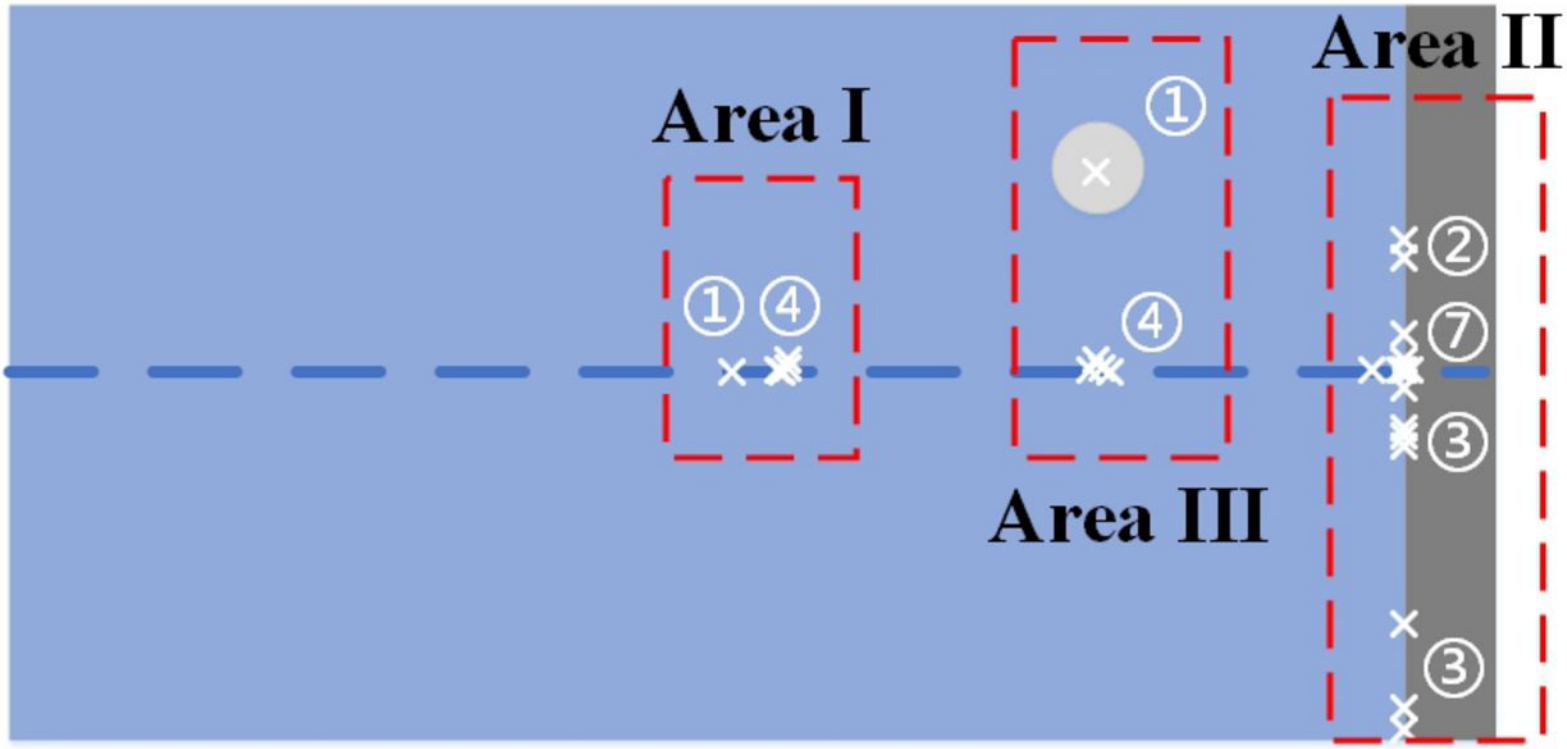

(a) Blade sample smeared with salt fog

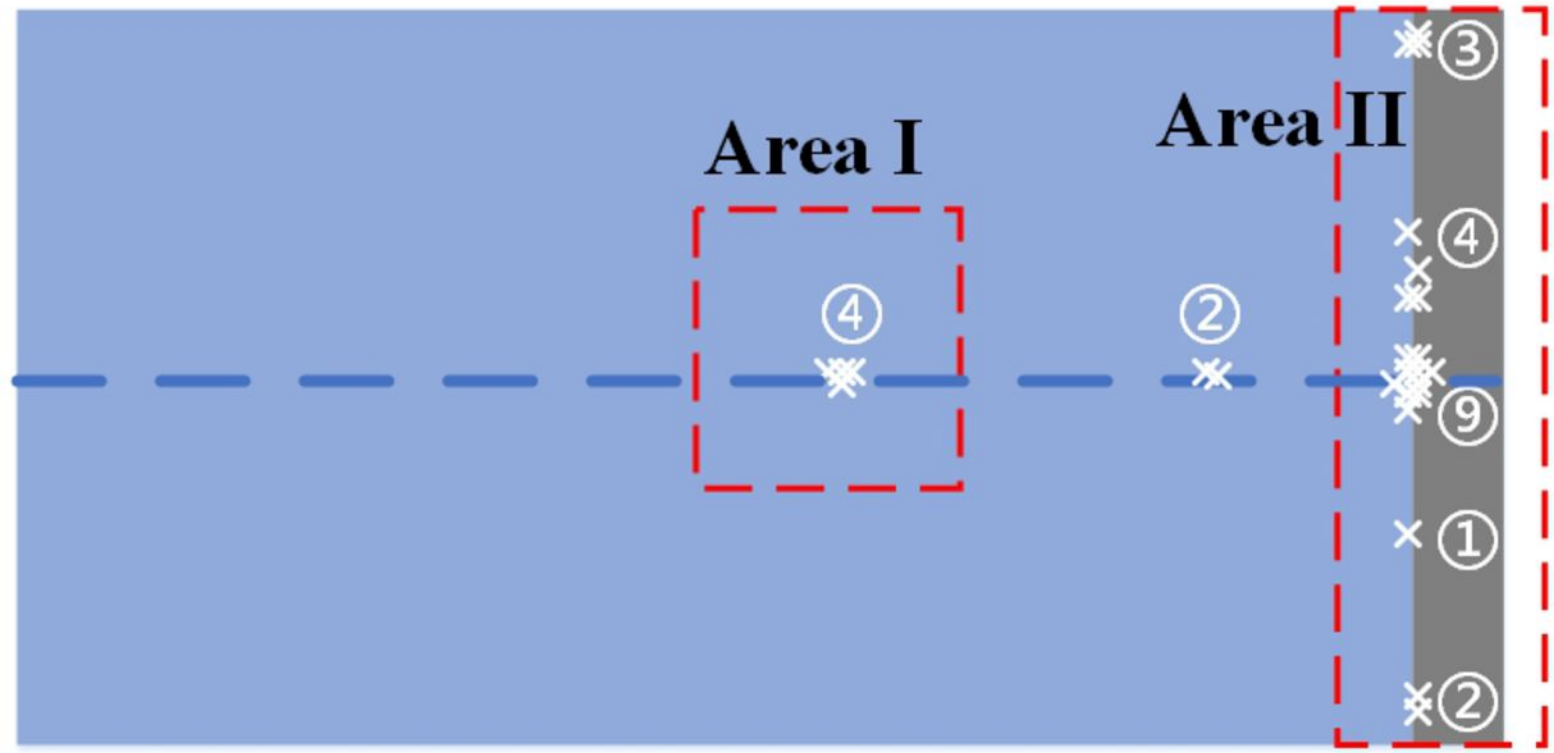

(b) Clean blade

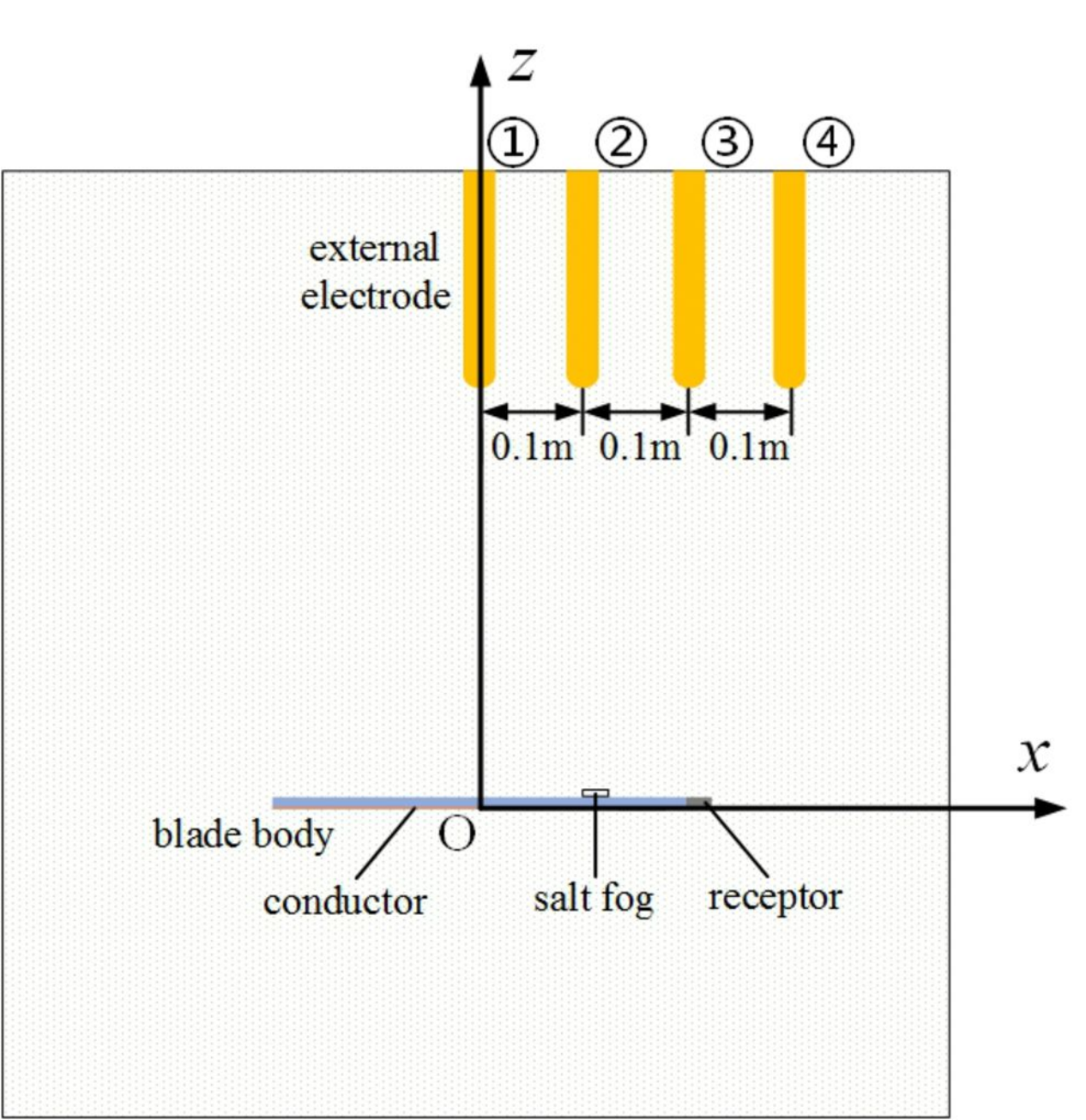
z
①
②
③
④
external
electrode
0.1m
0.1m
0.1m
x
blade body
O
conductor
salt fog
receptor

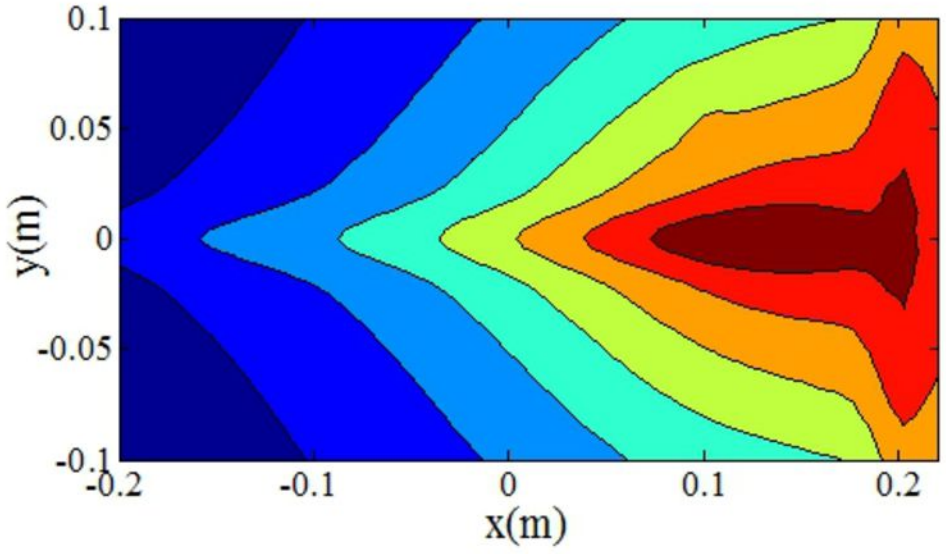

(a) LSP when $x_{ed} = 0$m

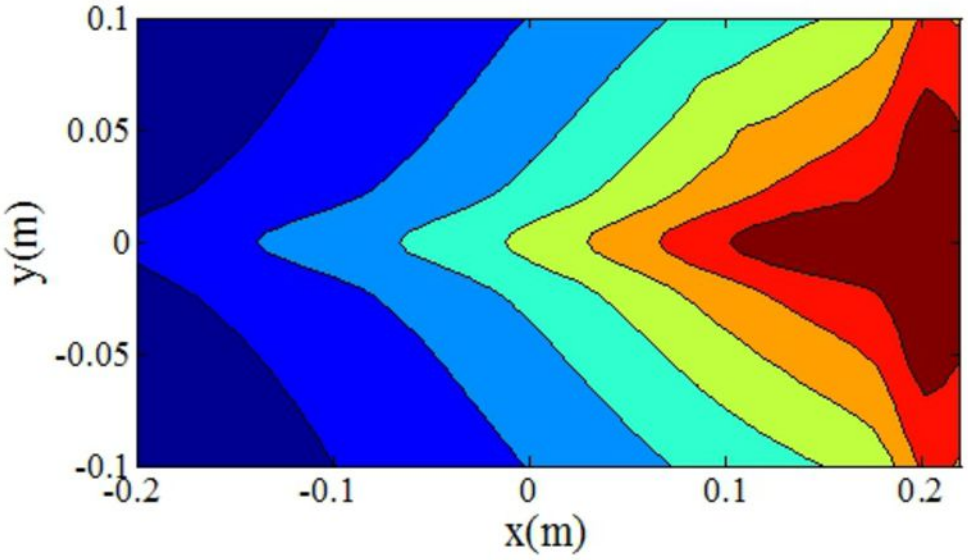

(b) LSP when $x_{ed} = 0.1$m

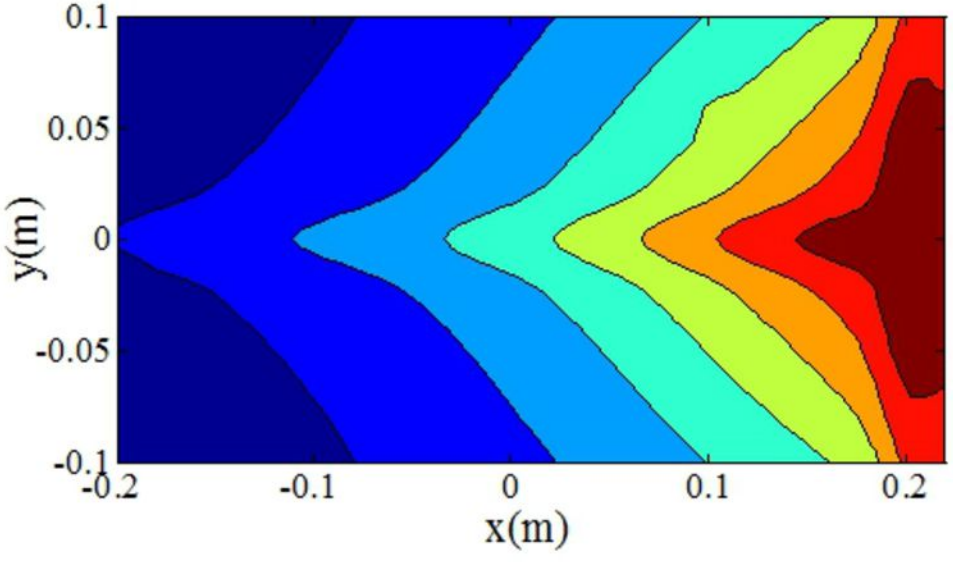

(c) LSP when $x_{ed} = 0.2$m

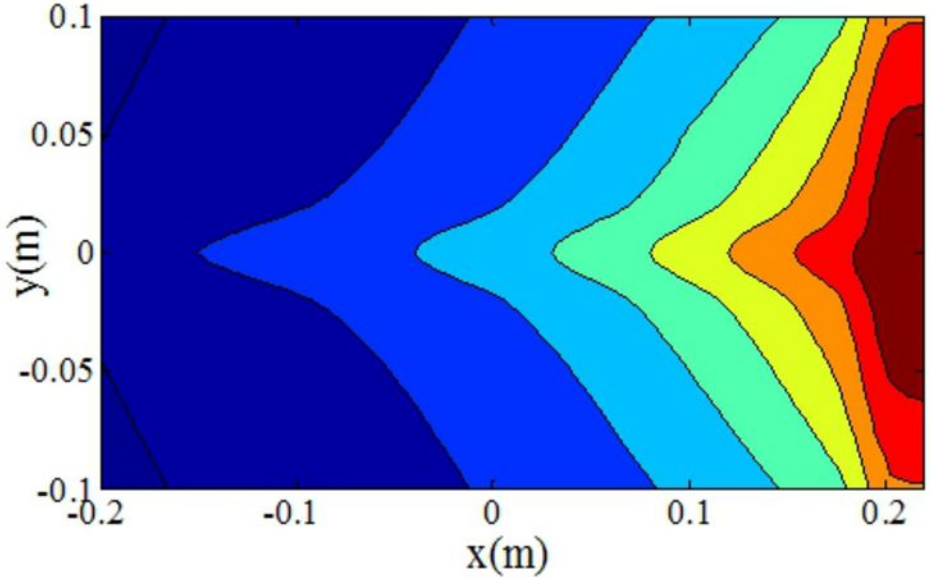

(d) LSP when $x_{ed} = 0.3$m

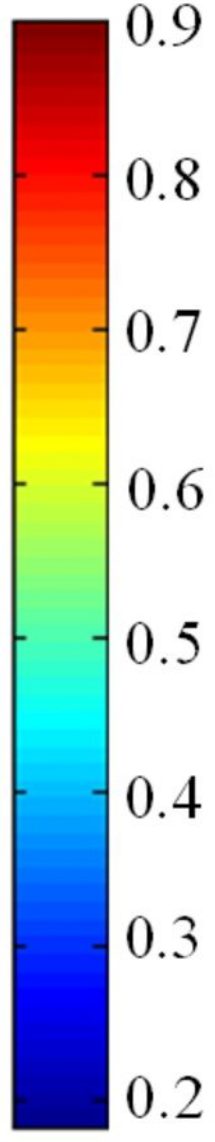

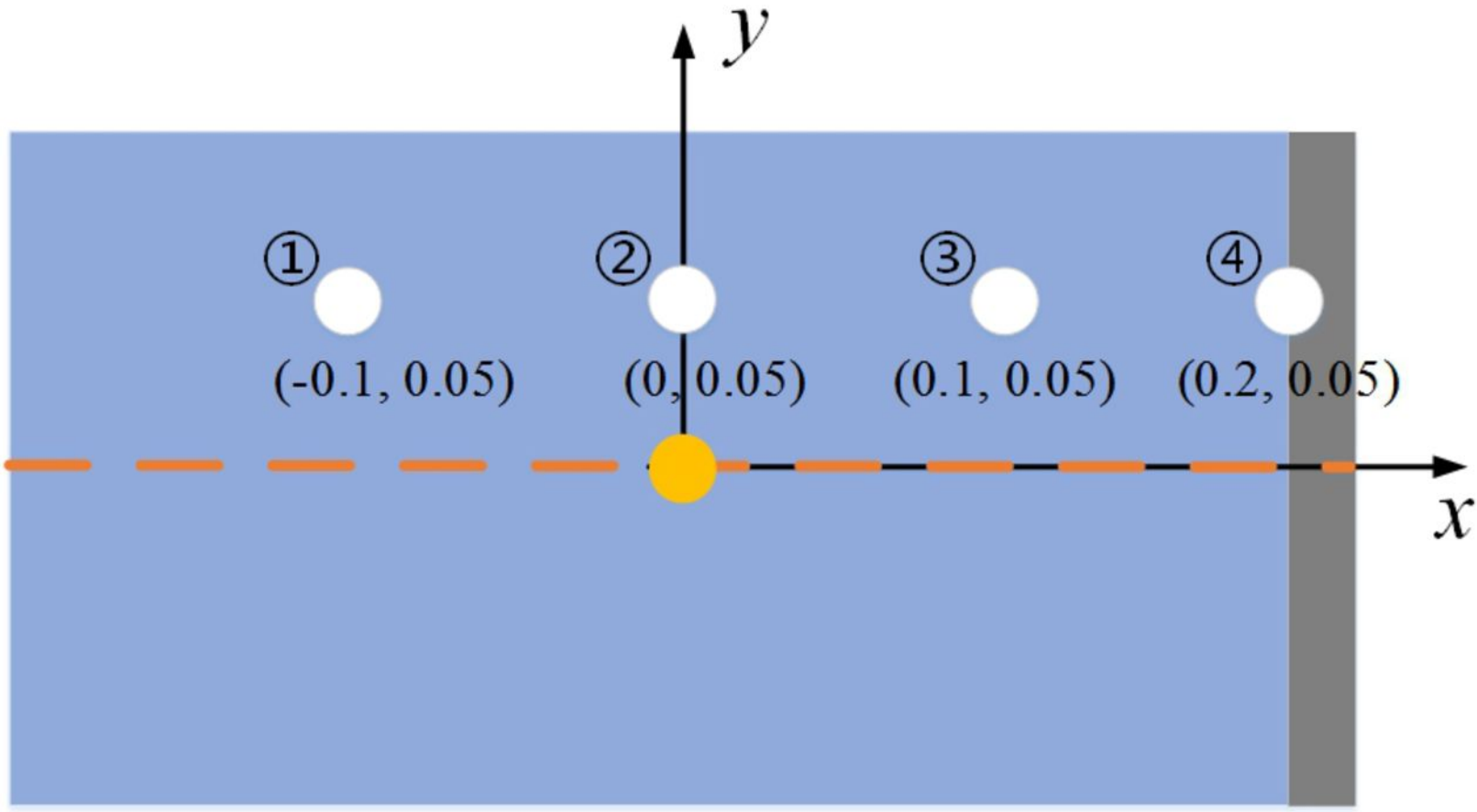
y
①
②
③
④
(-0.1, 0.05)
(0, 0.05)
(0.1, 0.05)
(0.2, 0.05)
x

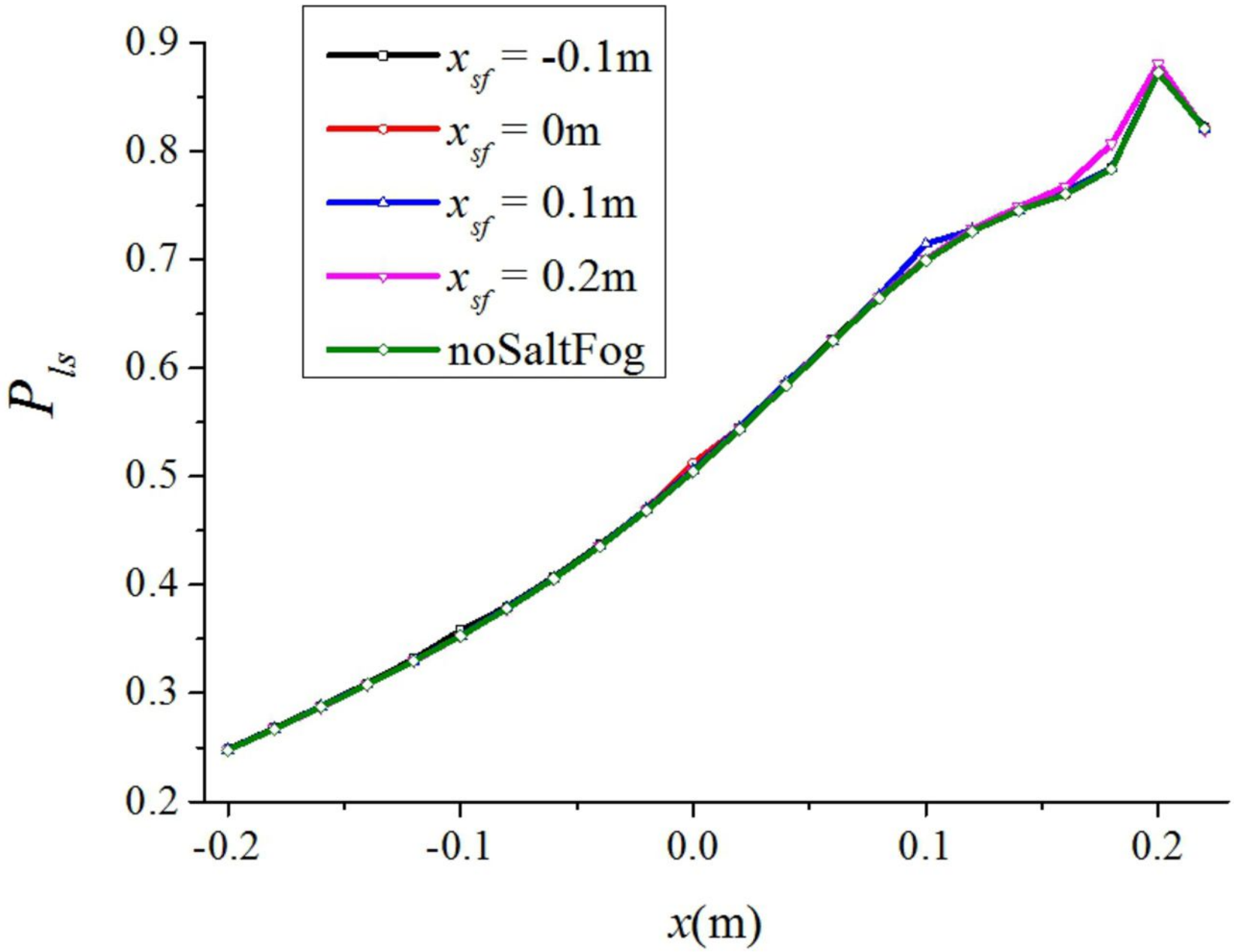
x_{sf} = -0.1m
x_{sf} = 0m
x_{sf} = 0.1m
x_{sf} = 0.2m
noSaltFog
P_{ls}
0.9
0.8
0.7
0.6
0.5
0.4
0.3
0.2
-0.2
-0.1
0.0
0.1
0.2
x(m)

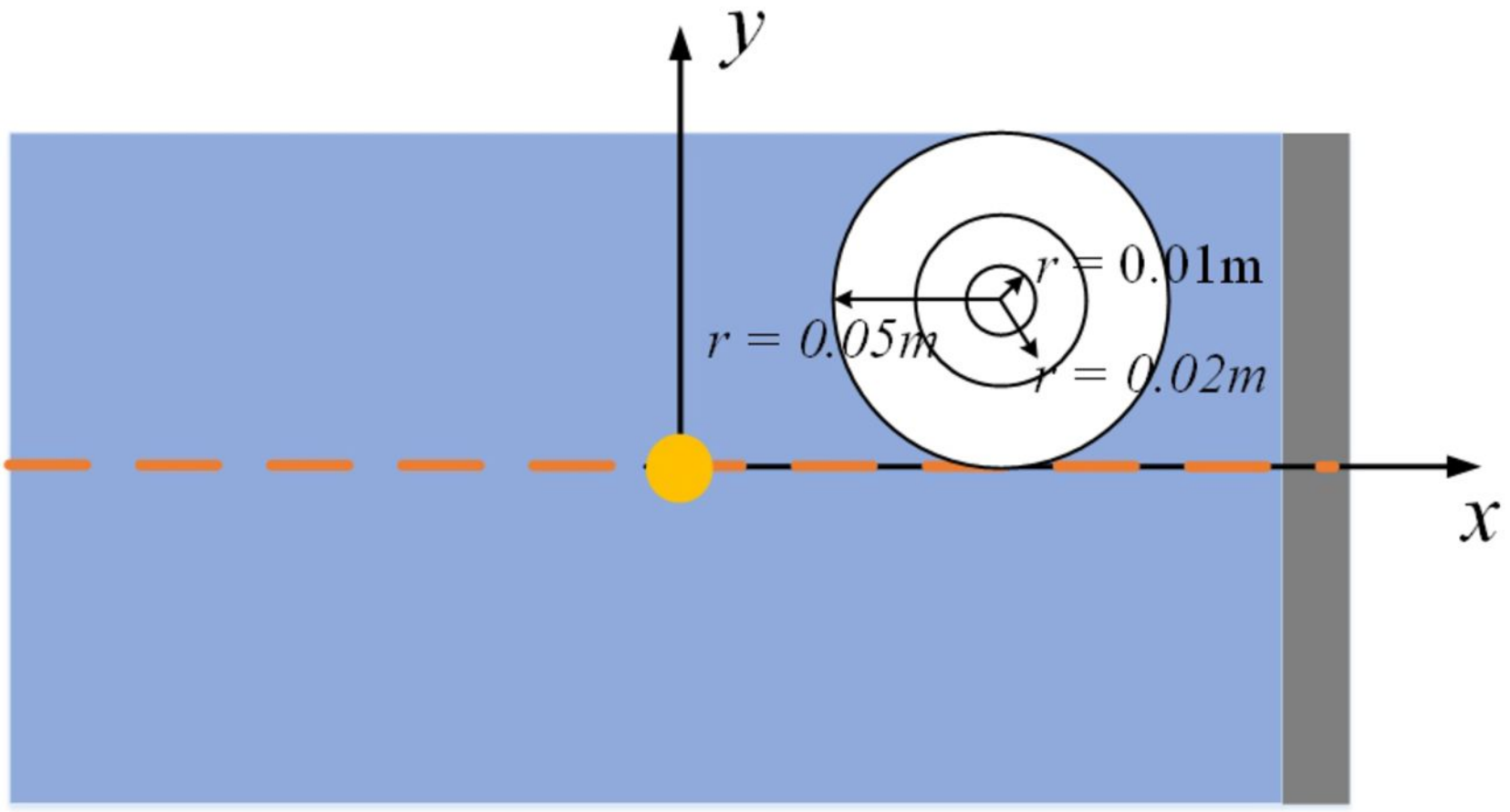
y
r = 0.01m
r = 0.05m
r = 0.02m
x

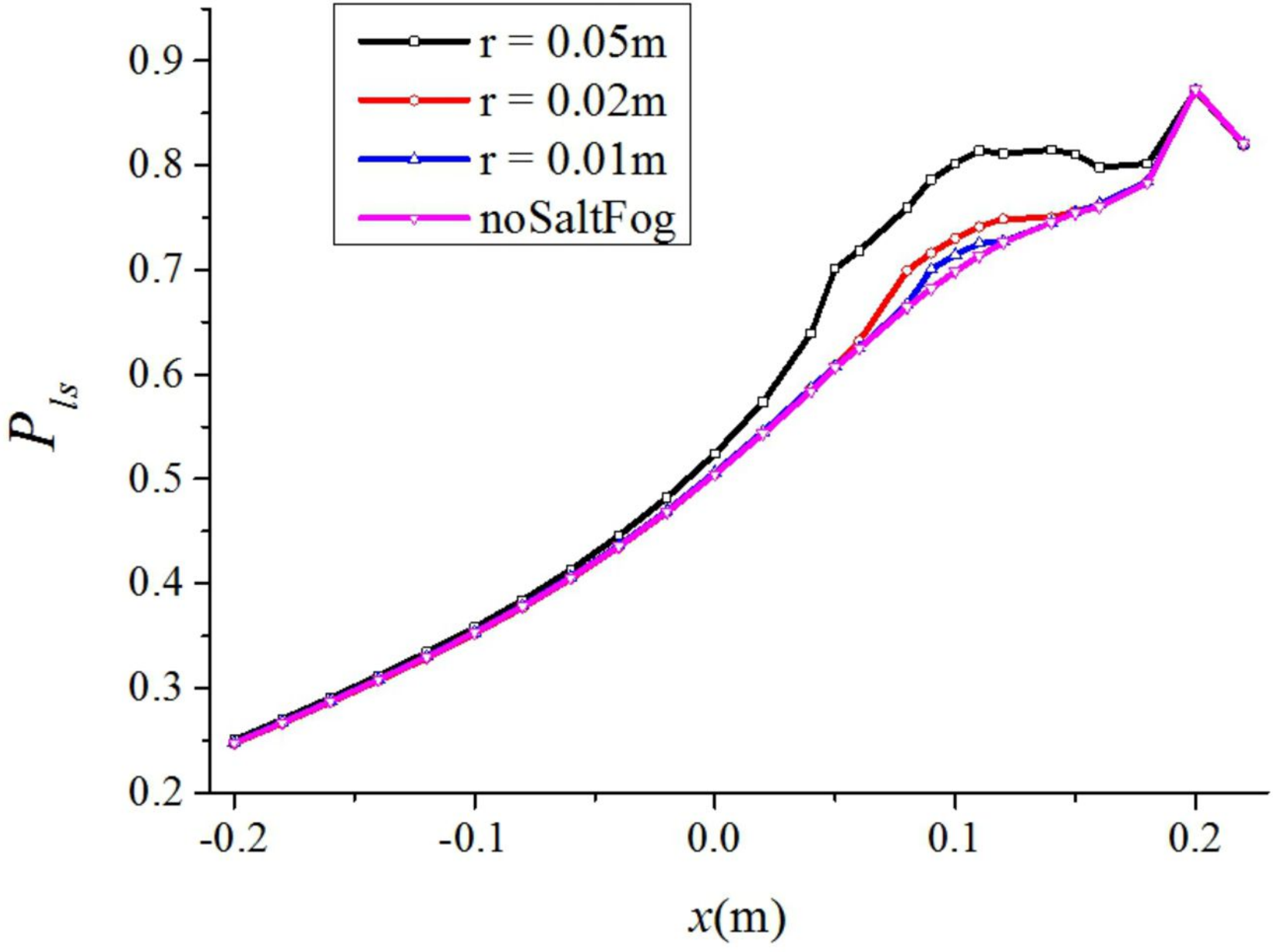
r = 0.05m
r = 0.02m
r = 0.01m
noSaltFog
0.9
0.8
0.7
0.6
0.5
0.4
0.3
0.2
P_{ls}
-0.2
-0.1
0.0
0.1
0.2
x(m)